EUROPEAN COMMISSION

Community Research

THERESA

(Contract Number: 036458)

Deliverable 12

Title of report:

THM Numerical Models

Authors:

Antonio Gens, Maria Teresa Zandarin

Date of issue of this report: **26/10/2009**

Start date of project: **1 January 2007** Duration: **36 Months**

Project co-funded by the European Commission under the Sixth Framework Programme Euratom Research and Training Programme on Nuclear Energy (2002-2006)		
Dissemination Level		
PU	Public	✓
RE	Restricted to a group specified by the partners of the THERESA project	
CO	confidential, only for partners of the THERESA project	

This page is intentionally left blank

Summary

This report constitutes Deliverable 12 of the THERESA project, financed by EC 6th FP Euratom in the field of radioactive waste management. It refers to the activities performed in Work Package 4 (WP4). As envisaged in the "Description of Work", the Deliverable deals with the application of the validated and improved computer codes and formulations to a large scale test. The Canister Retrieval Test (CRT) performed at the Aspo underground laboratory have been selected for this purpose.

From the test, two analyses, with different degrees of complexity were requested: i) a 1-D THM analysis focused on a section of the test at the canister mid-height, and ii) a full THM analysis of the entire CRT. In addition, the modelling teams were also asked to provide a steady state prediction of the full CRT system in order to provide information for the assessment of the capabilities of the computer codes regarding long term predictions. Based on the information contained in the reports contributed by the modelling teams, a number of significant modelling results are presented together with comparisons with field observations. The Deliverable ends with a series of concluding remarks concerning the performance of the models in this modelling exercise.

This page is intentionally left blank

Table of Contents **Page**

This page is intentionally left blank

1. Introduction

In the final phase of the Work Package 4 (WP4) activities, the improved and tested models developed during the lifetime of the project are applied to a large scale reference case. Among several options, the Canister Retrieval Test (CRT) was selected as the reference case during the Weimar meeting on May 31st 2007. There were several advantages in such a selection:

- The test achieved full saturation so the full process of hydration of the barrier could be modelled and compared with field observations.
- A large amount of data from the test was available concerning not only the time of running the tests but from the dismantling as well.
- There were gaps between barrier and heaters and between barrier and rock (filled with pellets) that provided the possibility of testing the models in presence of interfaces.
- The bentonite was present in two quite different forms: as compacted rings and cylinders and as pellets.

In this Deliverable, the main features of the CRT are presented first. From the test, two different analyses were proposed (Gens, 2008):

- A 1-D THM analysis focused on a section of the test at a canister mid-height
- A full THM analysis of the entire CRT

The 1-D analysis was thought to provide a good testing ground for the formulations and computer codes before embarking into the full scale analysis. The teams were also requested to provide a steady state prediction of the full CRT system in order to provide information for the assessment of the capabilities of the computer codes regarding long term predictions.

Results from the simulations of the various contributing teams for the set of analyses listed above are then presented. Only the most significant results have been selected for the report in order not to produce a too cumbersome document. The information has been obtained from the reports provided by the modeling teams: Bond et al. (2009) for Quintessa, Lempinen (2009) for Marintel, Millard and Barnichon (2009) for IRSN, Thomas et al. (2008, 2009) for Cardiff University (CU), Tong (2009) for KTH and Zandarín et al. (2008, 2009) for CIMNE. Although the Deliverable is of a descriptive nature, it concludes with some general remarks on the performance of the models in the modelling of a full-scale test.

2. Description of the Canister Retrieval Test.

A schematic view of the experimental geometry is given in Figure 2.1. More detailed drawings of the geometry of the CRT experiment are given in the CRT-Specifications (Gens, 2008) and in the description of Borgesson (2008).

The tunnel-profile has the approximate dimensions 6 × 6 m with a horseshoe-shaped profile. The experiments, CRT and TBT, are placed approximately at the tunnel centreline. The centre of the TBT experiment is located 6 m from the centre of CRT. In the CRT borehole, 16 filter mats with a width of 10 cm are installed with uniform spacing, 0.15 m from the borehole bottom up to 6.25 m height.

Ring-shaped or cylindrical bentonite blocks are placed in the borehole. At the top of the canister, bentonite bricks fill up the volume between the canister top surface and the top surface of the upper most ring (R10). The height difference between the two surfaces was 220 – 230 mm. The volume between the bentonite blocks and the borehole wall is filled with bentonite pellets and water.

An impermeable rubber mat was installed between bentonite block C4 and the concrete plug. On top of the plug a steel lid was installed. The plug and lid can move vertically and are attached to the rock by nine rock anchors. Because of the features of the design adopted, no friction between concrete plug and rock should be considered. Each of the nine rock anchors consists of 19 steel wires with a nominal area of 98.7 mm2. The inclination of the anchors is 2.5:1 or ≈ 22 °.

Summary from installation report.

The Canister Retrieval Test was performed to demonstrate the capability to retrieve deposited nuclear waste if a better disposal solution is found. The overall objective of the Canister Retrieval Test was to demonstrate to specialists and to the public that retrieval of canisters is technically feasible at any stage of the operating phase.

The CRT experiment has also been used to carefully record the THM processes in the Swedish KBS-3V deposit technique besides proving the possibility for retrieval of the canisters. This makes it very suitable for modellers to investigate theories, used in their simulations, since the calculated results can be checked against experimental data.

The test was installed in autumn 2000. The deposition tunnel for the experiment is located on the 420-metre level and is excavated by conventional drill and blast. The centre-to-centre distance between the two deposition boreholes is 6 metres, which is the spacing being considered for the deep repository, but only one of the boreholes has been used for this test (the other borehole was used to perform the TBT test). A maximum temperature of 100°C on the surface of the canister is aimed at for the Canister Retrieval Test.

The bentonite buffer was installed in form of blocks and rings of bentonite. The blocks have a diameter of 1.65 m and a height of 0.5 m. When the stack of blocks was 6 m high, the canister, equipped with electrical heaters, was lowered down in the centre of the borehole and the cables to the heaters and instruments were connected. Additional blocks were emplaced until the borehole was filled to a distance of one metre from the tunnel floor. The top of the borehole was sealed with a retaining plug made of concrete and a steel plate. The plug was secured against heave caused by the swelling clay with nine cables anchored in the rock. Water was supplied artificially for saturation around the bentonite blocks.

The deposition borehole for the Canister Retrieval Test was bored with a full-face tunnel boring machine modified for drilling vertical boreholes. The deposition borehole is 8.55 metres deep and has a diameter of 1.76 metres. The surrounding rock at the upper part of the borehole consists mainly of greenstone and the lower part of Äspö diorite. A 0.15 metre high concrete foundation was built to prevent the water leaking from the rock from reaching the bentonite blocks and to reduce the risk of tilting the stack of bentonite rings. Slots were cut in the rock wall for cables to prevent them from being damaged.

A canister obtained from SKB's Encapsulation Project was used for the Canister Retrieval Test. The outside diameter of the canister is 1,050 mm. The height of the canister is 4.83 m and the weight 21.4 tonnes. The bentonite used as buffer material is SKB's reference material, named MX-80. The buffer consists of highly compacted bentonite blocks and rings with an initial density of 1,710 and 1,790 kg/m3, respectively. The initial water content of the bentonite was 17%.

An artificial pressurised saturation system was built because the supply of water from the rock was judged to be insufficient for saturating the buffer. The pressurised saturation system provides a defined hydraulic boundary. The water is evenly distributed through a number of filter mats attached to the wall of the deposition borehole. A climate control system was used during installation to prevent the bentonite from being damaged by excessively high or low relative humidity.

A retaining structure is used to simulate a real storage situation. The aim of the structure is to prevent the blocks of bentonite from swelling uncontrollably. It consists of a concrete cone plug placed on top of the buffer and a steel lid which is pre-stressed by rock ties.

A large number of instruments are installed to monitor the test as follows:

- Canister – temperature and strain
- Rock mass – temperature and stress
- Retaining system – force and displacement
- Buffer – temperature, relative humidity, pore pressure and total pressure.

The data acquisition system consists of a measurement computer and dataloggers. The monitored values were transferred via a serial link from the dataloggers to the measurement computer. The computer was connected to Äspö data network.

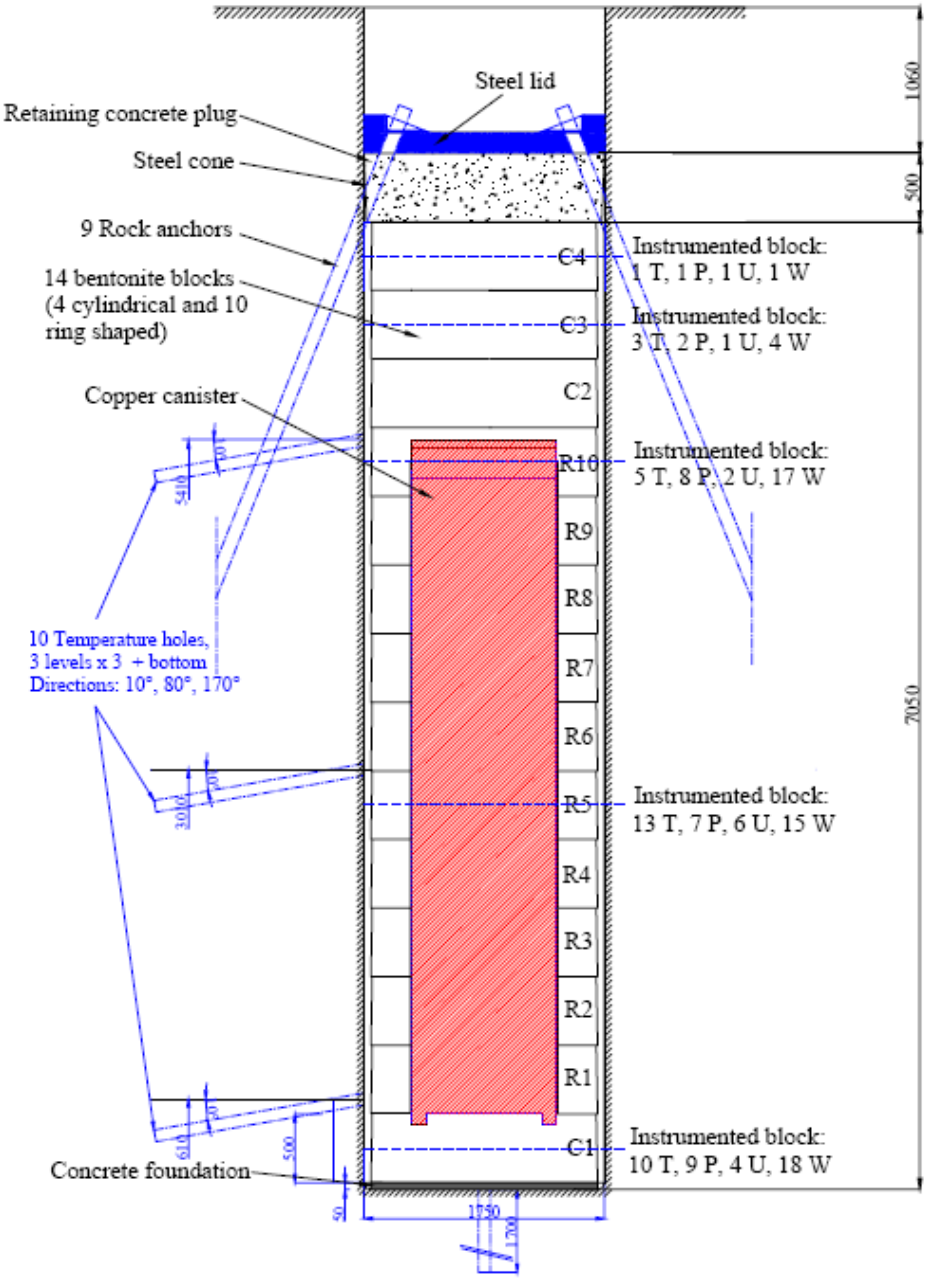

Figure 2.1 CRT geometry.

Test protocol

Since pellet filling marks the start of the test, the best description of the launching of the test is a step-by-step description of the procedures from that point in time:

1. Before the pellets were blown into the gap, instruments, heaters and wetting system installed were finished and the tubes for the drainage (pumping) system were removed along with the tubes and transducers for the ventilation system
2. Data collection was started immediately before pellet filling
3. The gap was filled with pellets on **October 26** ***(2000)***, which thus can be considered the starting date
4. Water was pumped into the gap and the filter mats, and the *(four)* water supply tubes were withdrawn immediately after *(during the)* pellet filling.
5. Measurement of water inflow into the filters started immediately after water filling
6. The rubber mat was placed on top of the upper block
7. The cable slots behind the conical ring were sealed with cement
8. The plug was cast when all preparations had been finished. Not more than 12 hours were allowed to pass between water filling and casting
9. Heating was started with an initially applied constant power of 700 W on October 27, i.e. one day after test start.
10. Three prescribed rods were locked on October 31 and the force and displacement transducers installed. *(At installation the force in the anchors were prescribed to 20 kN /anchor.)*
11. Between test start and locking of the rods (5 days) the plug rose 13 mm due to swelling of the bentonite.
12. The displacements and forces on the plug were carefully monitored
13. When the total force exceeded 1500 kN, the remaining rods were fixed in a prescribed manner. This procedure took place 12-14 December, i.e. 46-48 days after test start. *(When the average force in the three anchors exceeded 500 kN, the six remaining anchors were attached to the lid. The total force where distributed equally between all anchors, i.e. the force was ≈ 170 kN/anchor when all nine anchors were installed.)*
14. The canister heating power was raised twice: to 1700 W on November 13 and to 2600 W on February 13.
15. After the end of test, during it was dismantled several samples from the buffer were drilled to measured their dry density and degree of saturation.

In Tables 1, 2, 3 and 4 is presented a summary of the protocol following in the test.

Table 1. CRT heater power protocol

Date	Day	Heater Power [kW]	Comment
00-10-26	0	0	
00-10-27	1	0.7	
00-11-13	18	1.7	
01-02-13	110	2.6	
01-11-05	375	0	
01-11-06	376	2.6	
02-03-04	494	0	
02-03-11	501	2.6	
02-09-10	684	2.1	
03-12-04	1134	1.6	
05-03-10	1596	1.15	
05-10-11	1811	0	
06-03-28	1979	2	Testing the heaters
06-04-20	2002	0	

Table 2. TBT heater power protocol

Date	Day	Heater Power [kW]
00-10-26	0	0
03-03-26	881	0.9
03-04-03	889	1.2
03-04-10	896	1.5
06-06-09	2052	1.6

Table 3. CRT filter water pressure protocol.

Date	Day	Water pressure [MPa]	Comment
00-10-26	0	0	
02-09-05	679	0	Started to increase the water pressure gradually
02-10-10	714	0.8	
02-12-05	770	0.1	
03-01-09	805	0.4	
03-01-23	819	0.8	
05-03-12	1598	0	
05-12-16	1877	0	Air flushed

Table 4. Overview of rock anchor history.

Date	Day	Comment
2000-10-31	5	Three pre-stress anchors were attached to the lid. The initial force in each anchor was 20kN
2002-12-12 2002-12-14	46-48	The remaining six anchors were attached to the lid when the total force exceeded 1.5 MN. The total force was distributed evenly between the anchors, which give ~170kN/anchor. The force in three of the anchors has been measured.
2006-01-16 2006-01-18	1908-1910	The rock anchors were removed and the steel lid and concrete plug was lifted up from the deposition hole.

3. Canister Retrieval Test simulations.

Two simulations for Canister Retrieval test were carried out by the WP4 groups. The first one is a 1-D thermo-hydro-mechanical simulation of the mid-height section of the CRT (section 3.1). The second one is a full THM modelling of the CRT (section 3.2). Continuation of the analysis up to steady state conditions was requested for the full THM modelling.

3.1. Thermo-hydro-mechanical simulation of the engineered buffer at canister mid-height section.

In this task a disk of the engineered buffer, consisting of a gap close to the canister, a ring-shaped bentonite block and a pellet-filled outer gap, located at canister mid-height is to be simulated considering thermal, hydraulic and mechanical processes. Thermal boundary conditions can be obtained from the thermal 3D simulation or from experimental data.

3.1.1 Description of the case

Geometry

This task is focused on the mid-section of the buffer. A disc of the engineered buffer is to be modelled, rotational symmetry can be assumed, see Figure 3.1.1
A radial-symmetric model can be used, where the model should contain:

A. the inner gap (0.01 m width)

B. the ring shaped bentonite block

C. the outer gap filled with bentonite pellets (0.055 m width)

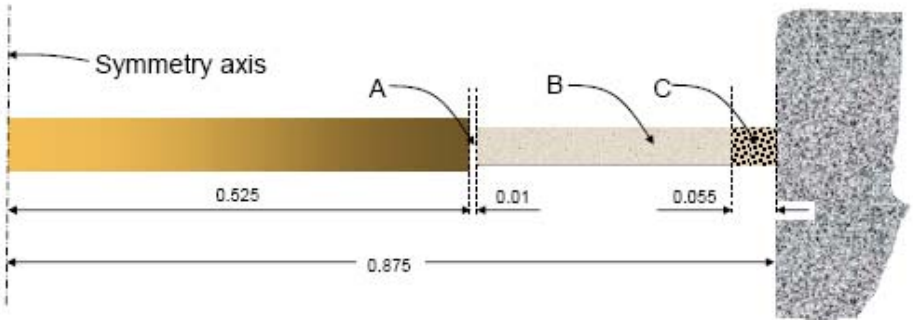

Figure 3.1.1 Geometry of the mid-section.

Boundary conditions

Suggested boundary conditions of the selected disk of the engineered buffer are given in Table 5. The canister temperature data is however incomplete since the sensors

broke down after approximately 1000 days. Therefore the simulated temperature and heat flux are also available (Figure 3.1.2). The temperature in the rock wall boundary is given in Figure 3.1.3 and the initial conditions of the material are summarised in Table 6.

Table 5. Suggested boundaries conditions.

	Type of process		
Boundary	Thermal	hydraulic	Mechanical
Canister	Mid-heigth heat flux (only suitable if your model has a small radial dimension as compared to the canister height) or temperature from 3D simulation or temperature from experimental data Sensor P12.	Zero water flux	Roller condition
Horizontal	Zero thermal flux	Zero water flux	Roller condition
Hole wall	Temperature from 3D simulation or experimental data Sensor TR125.	Water pressure from filter pressure protocol	Roller condition

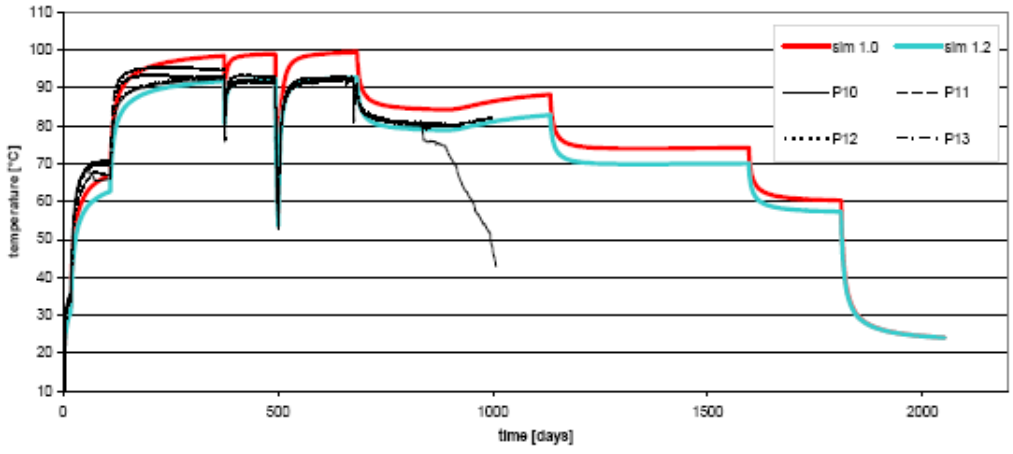

Figure 3.1.2 Experimental and simulated canister surface temperatures at canister mid-height.

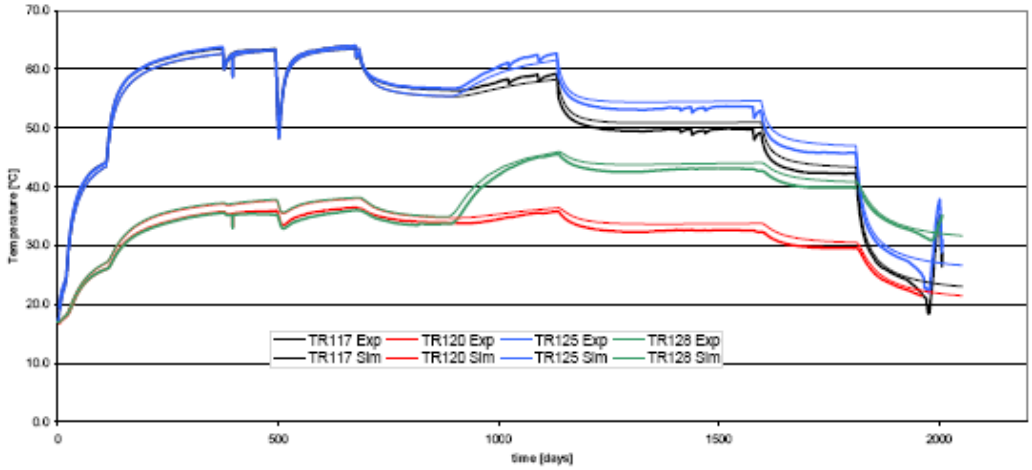

Figure 3.1.3. Experimental and simulated rock temperatures at canister mid-height.

Table 6. Initial conditions

	Type of process		
Section	Thermal	Hydraulic	Mechanical
A. Inner gap	T=20 ºC	S_r=0-1? (is it filled)	s=0MPa, *n*=1
B. Bentonite block	T=20 ºC	S_r=0.859	s=0MPa, *n*=0.36
C. Pellet-filled gap	T=20 ºC	S_r=0.895	s=0MPa, *n*=0.64

Results requested

The experimental data for comparison were provided in the form of excel-files. The selected set of data points, defined as a position of a material particle in the initial (undeformed) configuration, are shown in Figure 3.1.4.

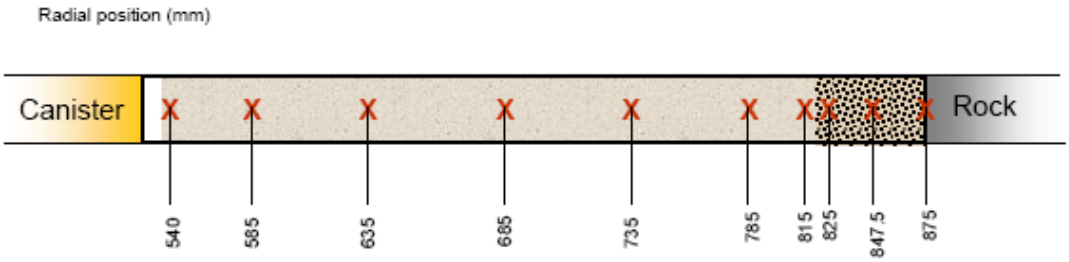

Figure 3.1.4: Schematic drawing of the points where variable histories should be presented. The radial distances are given in the initial (undeformed) configuration.

3.1.2 Results obtained by the modelling groups.

A. CIMNE (Code_Brigth)

The geometry used for simulation is axi-symmetric and three materials were considered (Figure 3.1.5): gap, bentonite and pellets. The geometry is discretized by 4-noded quadrilateral structured elements, and the mesh includes 51 elements and 104 nodes.

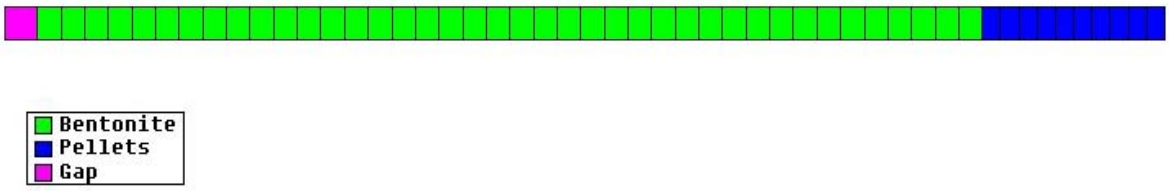

Figure 3.1.5: Mesh and materials considered in the simulation.

The thermo-hydro-mechanical parameters of the bentonite were adopted from the CRT-Specifications. The parameters for pellets were adjusted by back analysis. The hydraulic parameters of the gap were adopted to allow quick drainage of the water filling it.

The comparison of values measured and calculated is presented in Figures 3.1.6 to 3.1.9. The final state of the buffer is plotted in Figure 3.1.10. And the evolution of the aperture and horizontal stress of the gap are shown in Figure 3.1.11.

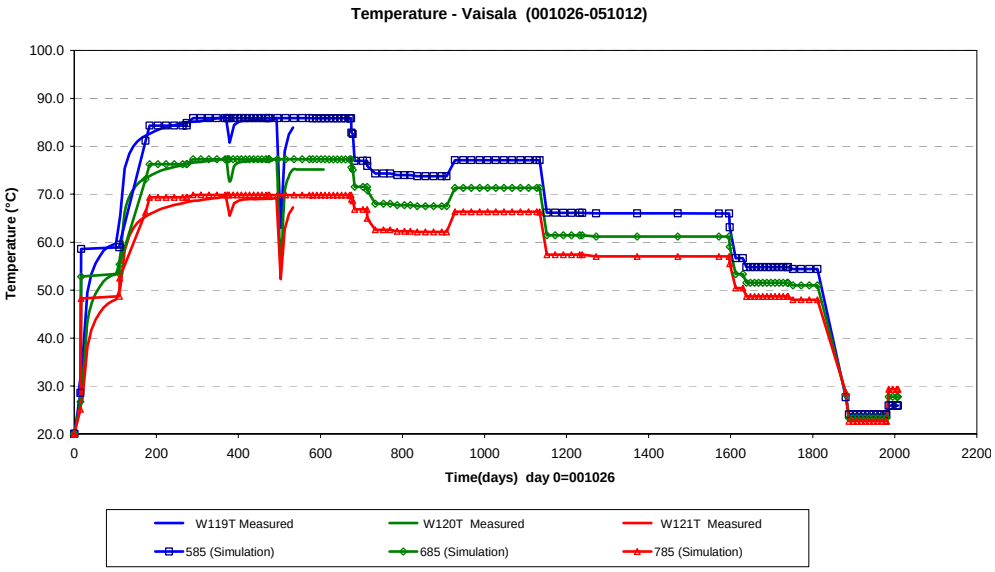

Figure 3.1.6: Comparison between temperatures, calculated and measured by Vaisala sensors

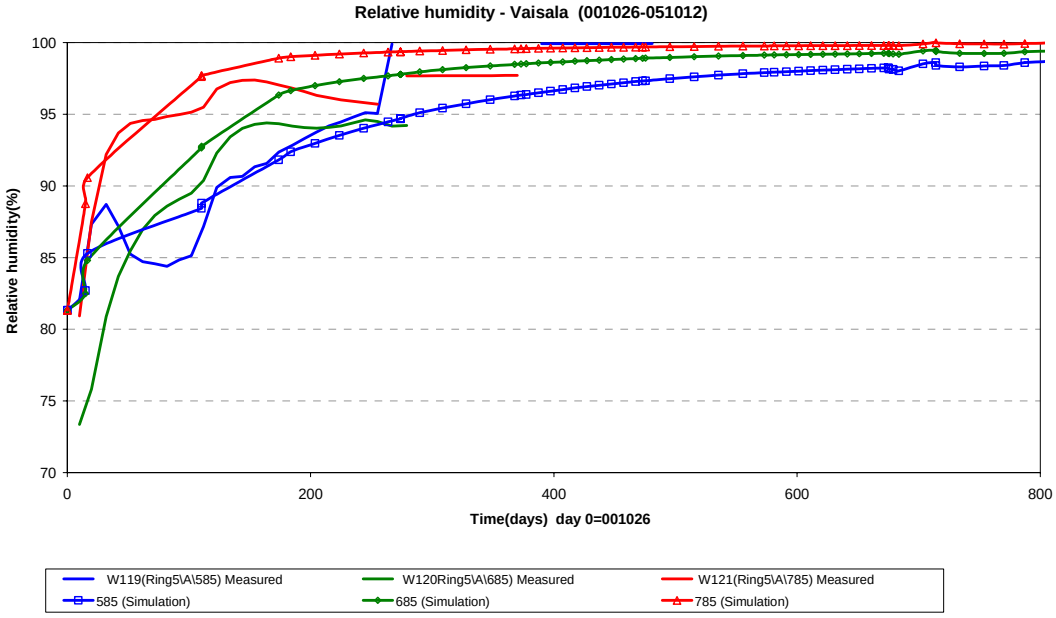

Figure 3.1.7: Comparison between relative humidities, calculated and measured by Vaisala sensors

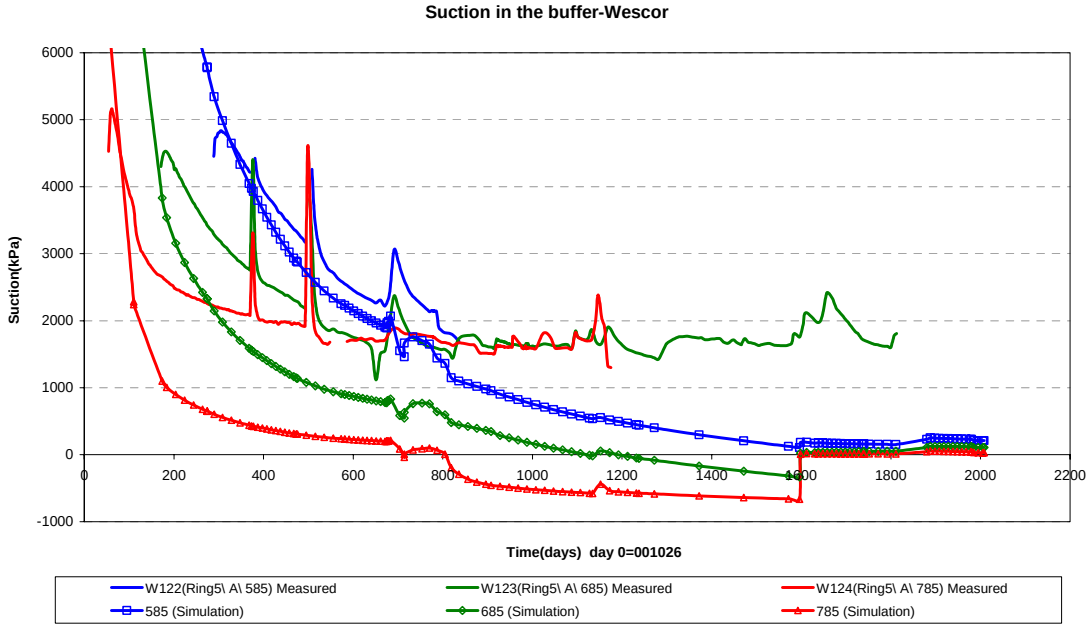

Figure 3.1.8: Comparison between calculated and measured suctions.

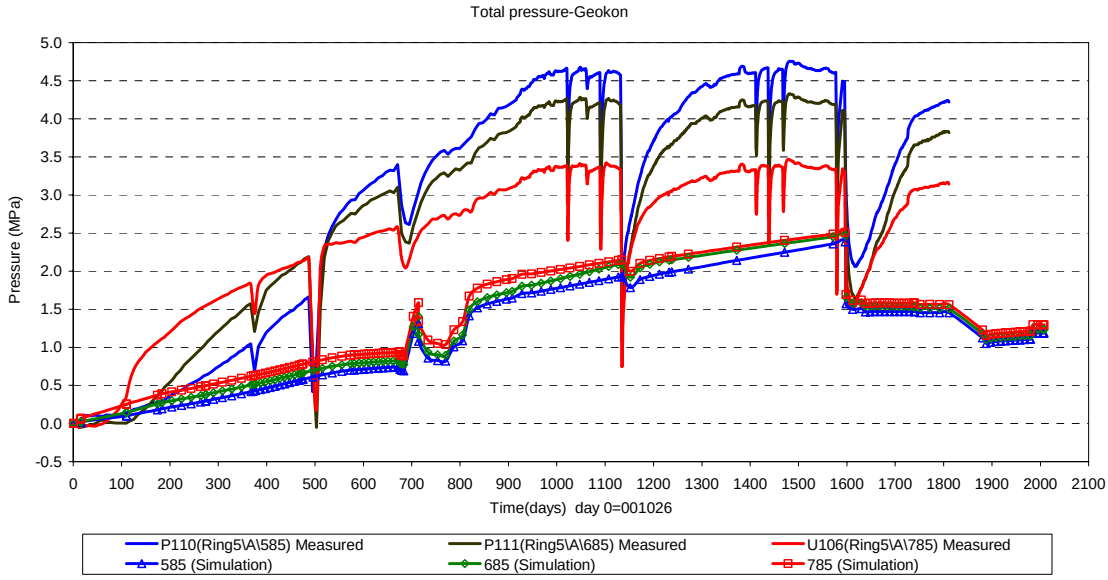

Figure 3.1.9: Comparison between measured and calculated total axial stresses.

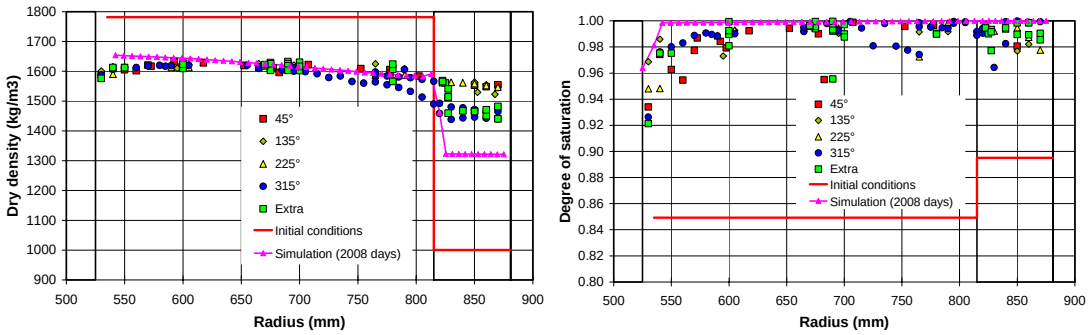

Figure 3.1.10: Dry densities at the end of simulation (2008 days) (left). Degree of saturation at the end of test (right).

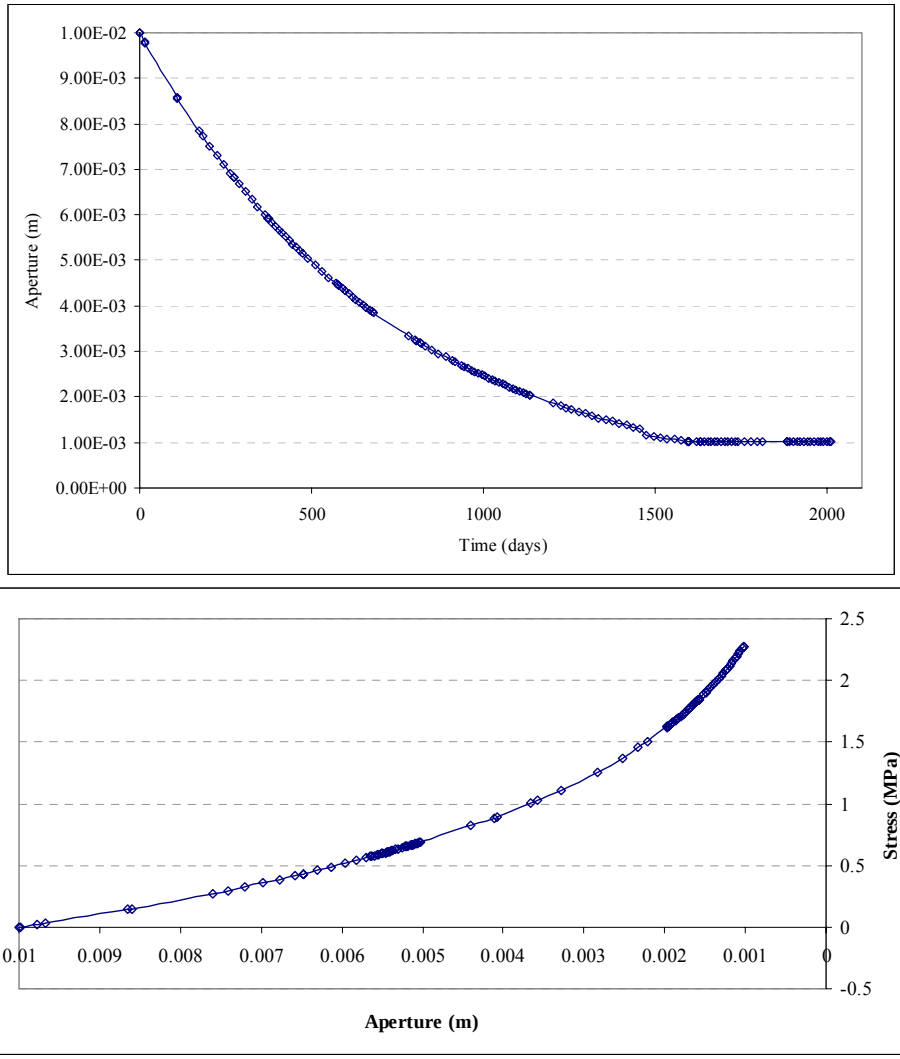

Figure 3.1.11: Evolution of the aperture of the gap (top) and horizontal stress (bottom).

B. Posiva/Marintel (Free Fem++)

1-D CRT simulation not reported.

C. KTH (ROLG)

A 3D ring model was used for the simulation because code ROLG has no functionality for axisymmetric problems. The model geometry is equivalent to a ring model with the inner radius equal to 535 mm and the outer radius equal to 875 mm. Hexahedron elements are used to build the 3D FEM mesh. The number of nodes is 1260 and the number of elements is 1200.(Figure 3.1.12). The gap between canister and buffer was treated as interface elements. The gap between bentonite and rock was

treated as solid bentonite elements with material properties different from standard MX-80, since they were filled with pellets of bentonite.

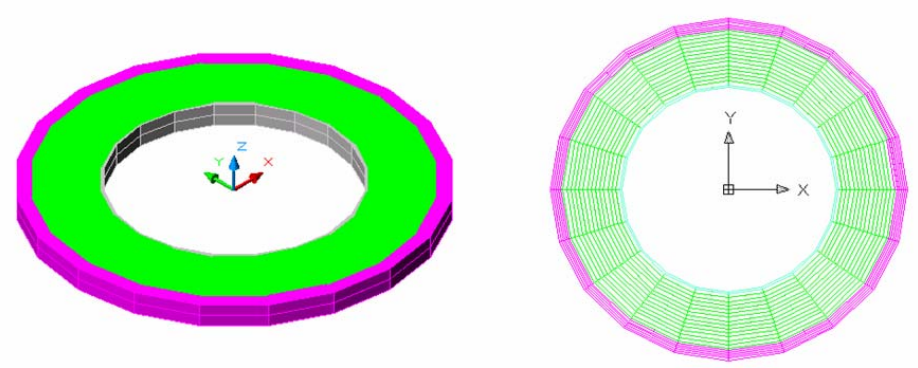

Figure 3.1.12 3-D FEM mesh. The elements with pink colour represent the outer gap of filled pellets

An interface element was incorporated in the code to study this case. The normal stiffness of the element is taken as a function of normal displacement. And the shear stiffness is assumed constant.

The comparisons between measured and calculated data are given in Figure 3.2.13 to 3.2.15. The final dry density of the buffer is given in Figure 3.2.16. And the evolution of the aperture of the gap is plotted in Figure 3.2.17.

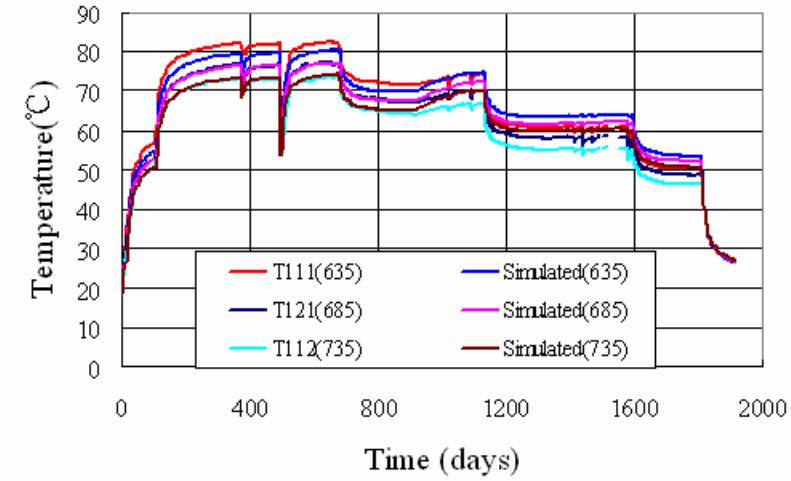

Figure 3.1.13 Comparison between simulated and measured temperatures.

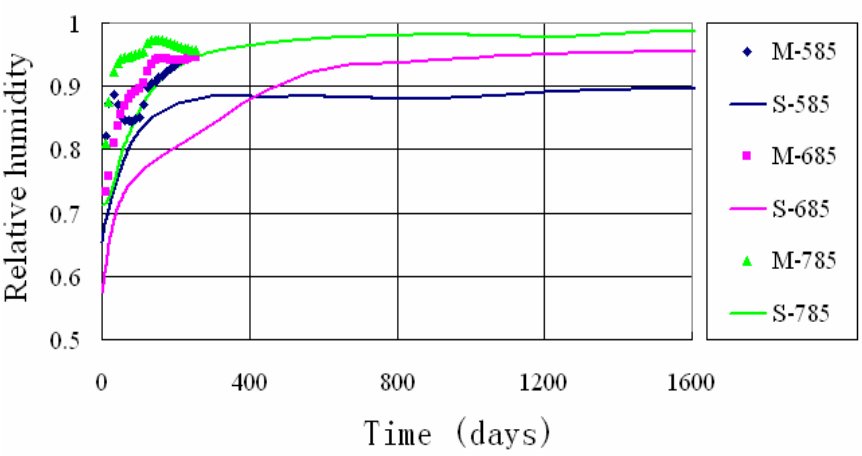

Figure 3.1.14 Relative humidity comparisons

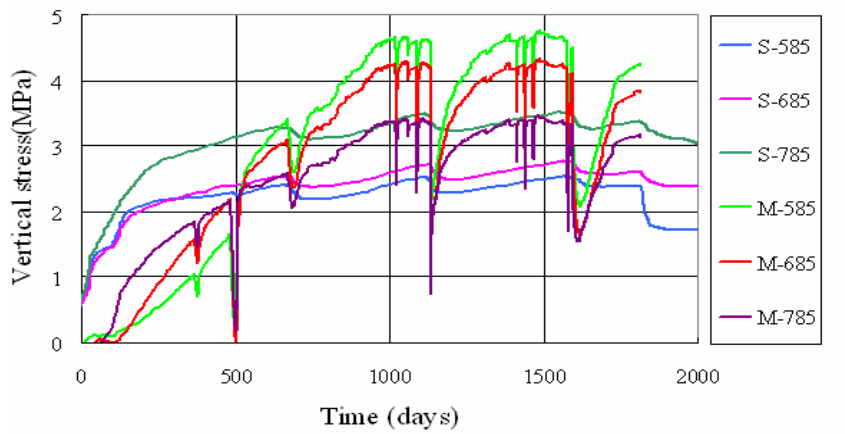

Figure 3.1.15 Comparison between the simulated (with letter S in the legend) and measured (with letter M in the legend) vertical stress

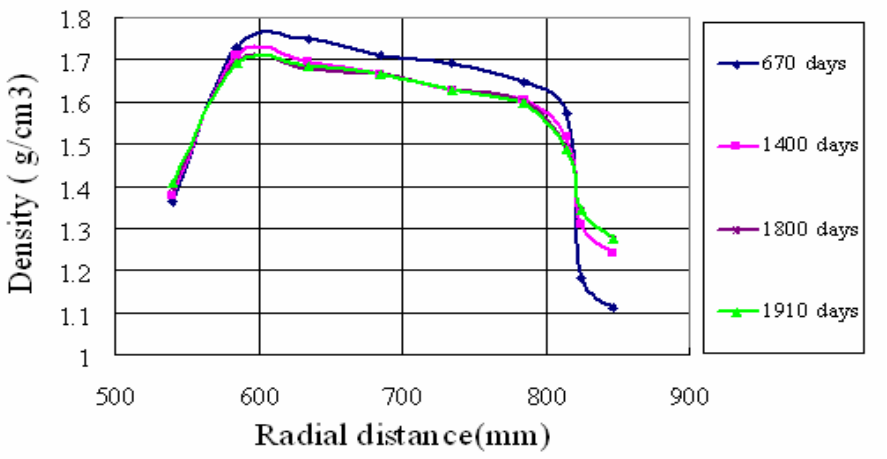

Figure 3.1.16 Simulated dry density profiles at different times

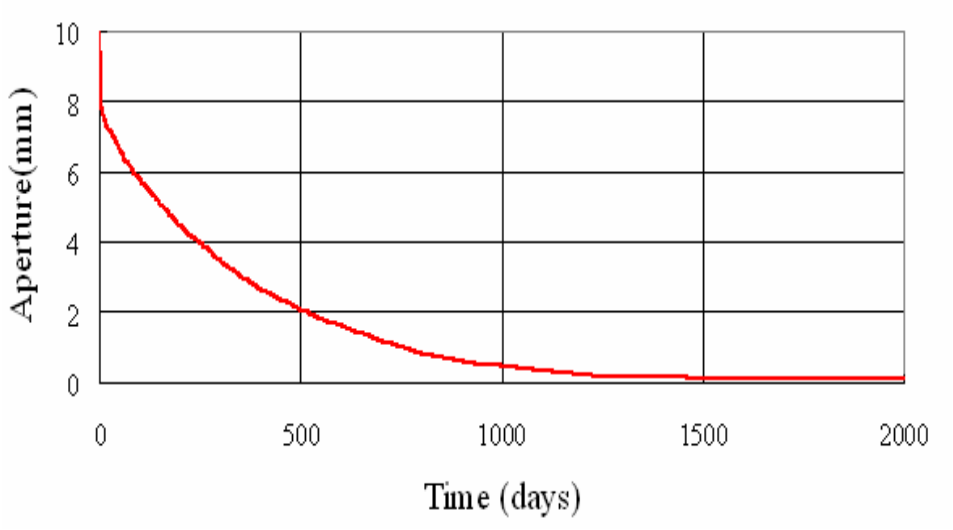

Figure 3.1.17 Variation of gap aperture vs. time

D. Quintessa (QPAC-EBS)

The discretized geometry is shown in Figure 3.1.18. It was assumed that the annulus between the bentonite and canister was full of water, and hence the water available for ingress was equal to the plan area of the gap annulus multiplied by the vertical height of the 1D model. Should the inner boundary of the bentonite come into contact with the canister before all available water is used up, the boundary becomes 'no-flow' as it is assumed that all the available water has been squeezed out elsewhere in the system. Note that because of the very high suctions in bentonite and the small volume of the air gap annulus, it is expected that the water will be taken up extremely quickly. In order to represent the observed mass redistribution, the properties of the pellets were taken to be different from those of the bentonite ring. The pellets were assumed to be mechanically weak as the secondary porosity associated with the pellets was reduced, but as the pellet total porosity approached that of the bentonite rings the pellet mechanical properties tended to those of the bentonite rings.

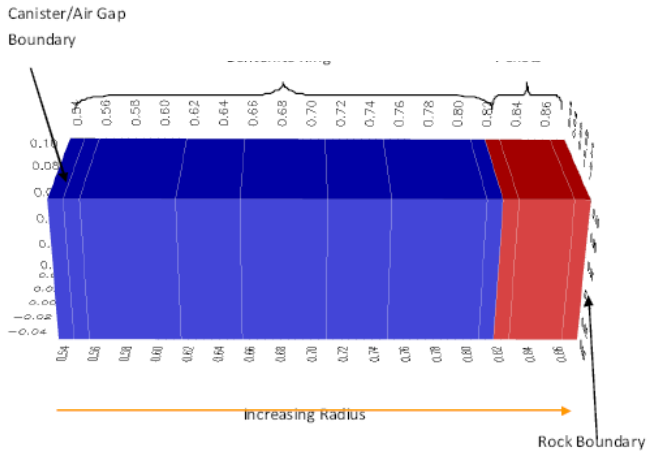

Figure 3.1.18: 1-D Discretisation

The comparisons between measured and calculated data are presented in Figures 3.1.19 to 3.1.21. It can be noted that the computed stresses (Figure 3.1.21) are quite high in comparison with the data. This was because the 1D case caused an artificial restriction in the vertical direction (hence higher stresses), which were not so evident in the 3D case. The final state of buffer is given in Figure 3.1.22.

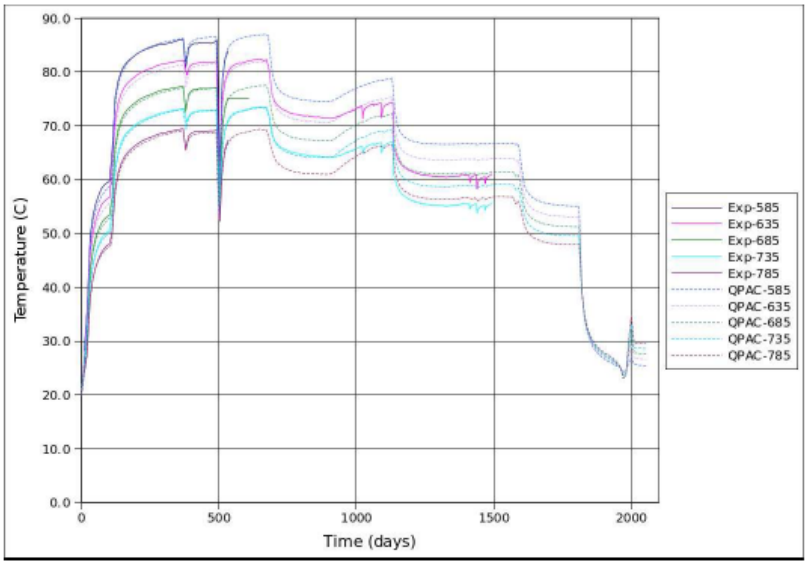

Figure 3.1.19: Comparisons between calculated and measured temperature evolutions

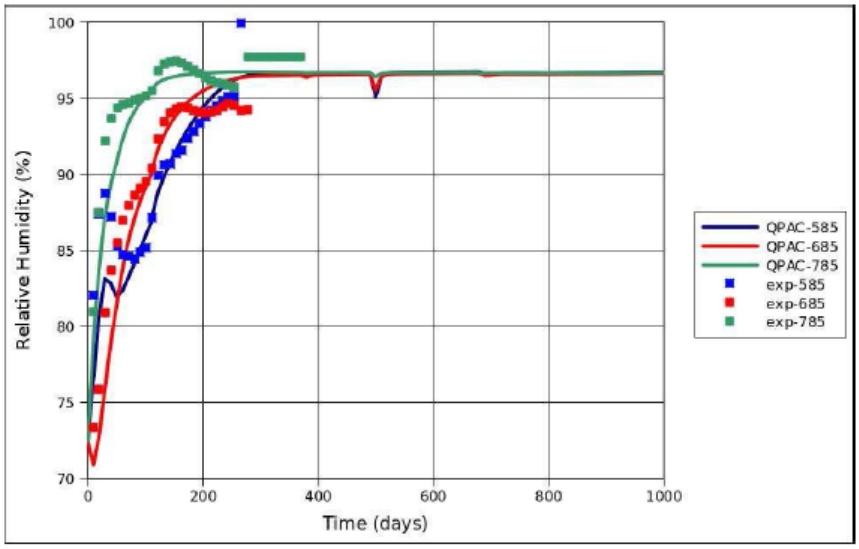

Figure 3.1.20: Comparisons between calculated and measured relative humidity evolutions

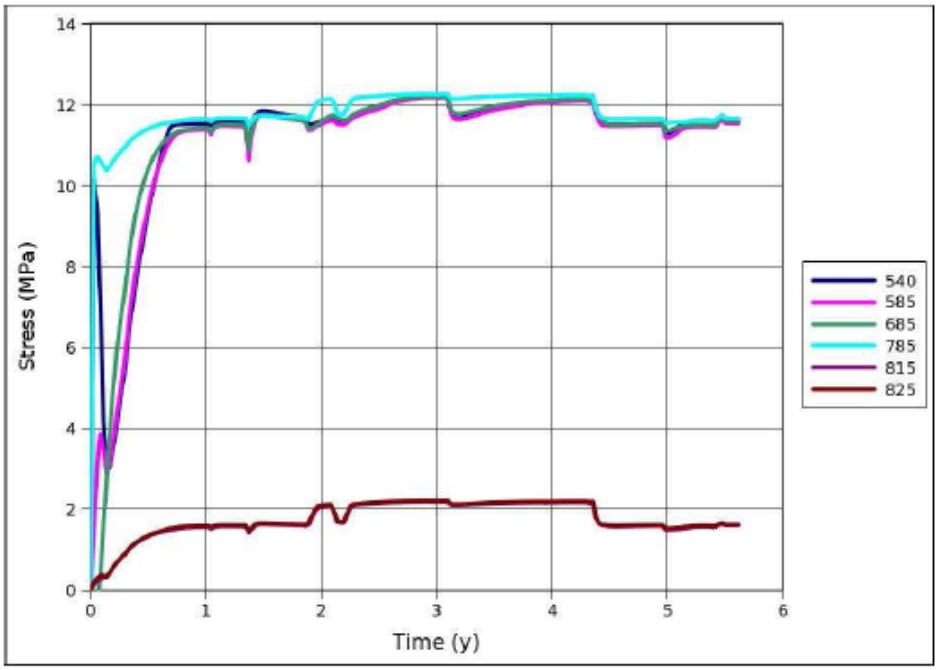

Figure 3.1.21: Calculated evolution of axial stresses.

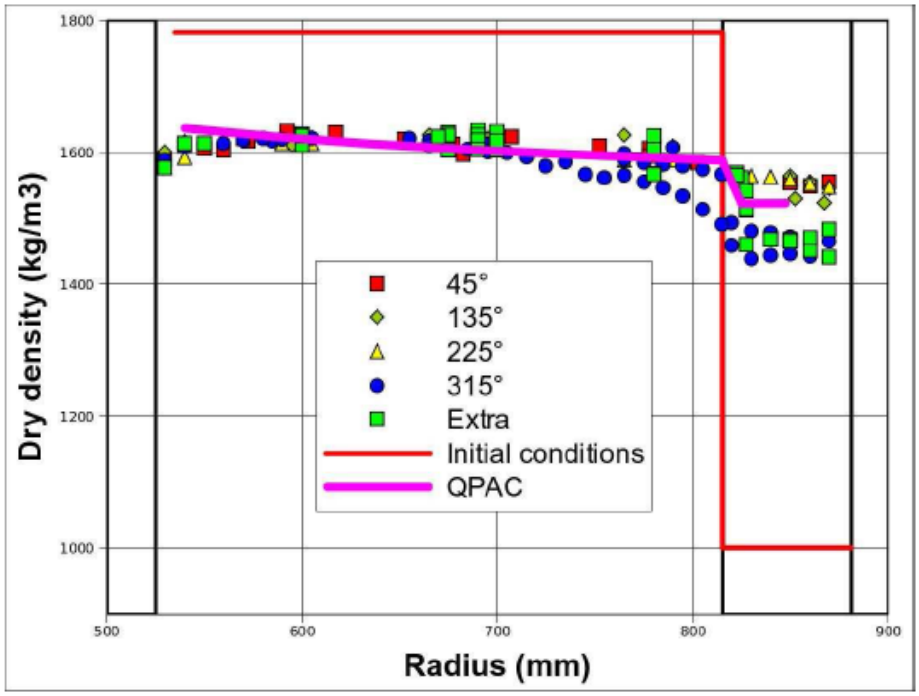

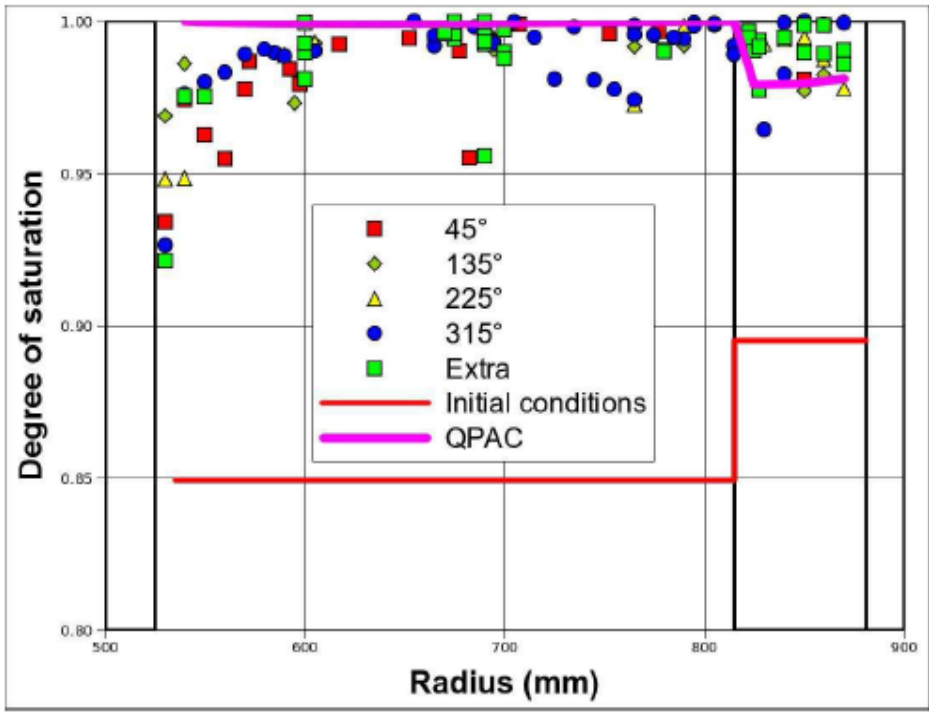

Figure 3.1.22: Comparisons between calculated and measured bentonite dry density at the end of the experiment (top) .Comparisons between calculated and measured degrees of saturation at the end of the experiment (bottom)

E. CU (COMPASS)

A 1D axisymmetric domain was used for the numerical analysis. A mesh consisting of four-noded isoparametric elements was used, with the bentonite buffer discretised into 100 elements and the gap filled with bentonite pellets discretised into 20 elements, as shown in Figure 3.1.23. The 0.01 m air gap was considered negligible due to the highly swelling nature of the MX-80 bentonite. A time step of 1000 seconds has been found to yield converged results.

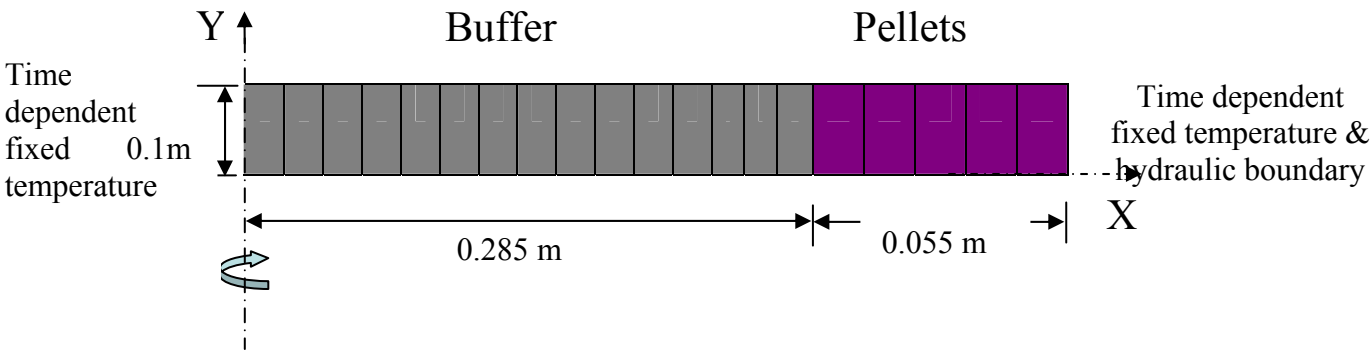

Figure 3.1.23: Schematic diagram of 1D axisymmetric mesh (100 elements for bentonite buffer, 20 elements for gap filled with bentonite pellets)

Figure 3.1.24 compares the thermal distribution results obtained numerically to those measured experimentally. Figure 3.1.25 presents the moisture distribution results in terms of relative humidity. Figure 3.1.26 presents the degree of saturation across the sample at various times. The whole buffer gets 100% saturated after 1000 days. Finally, Figure 3.1.27 compares the vertical (axial) stress results determined numerically and measured experimentally.

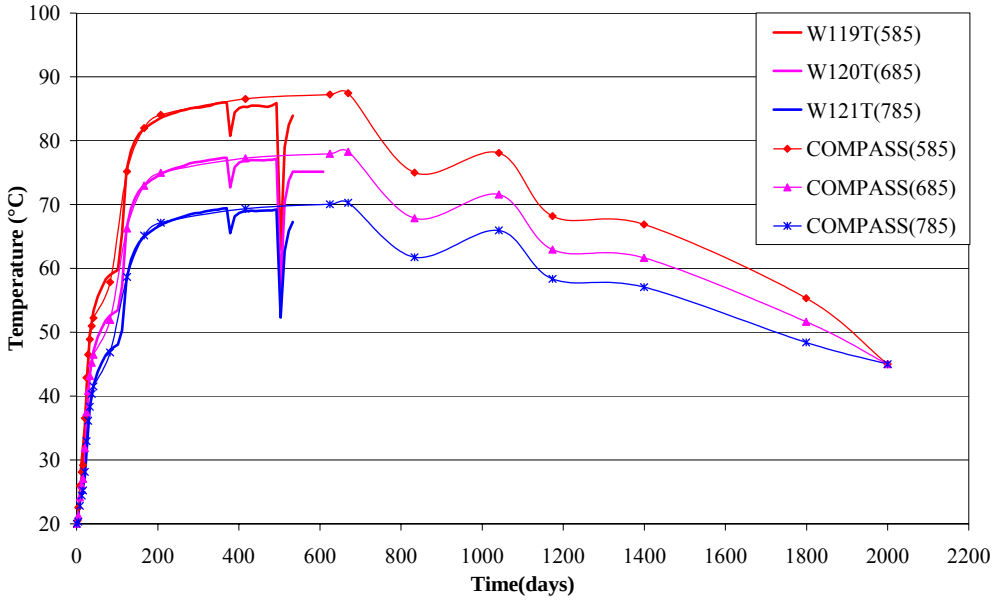

Figure 3.1.24: Comparison of temperatures

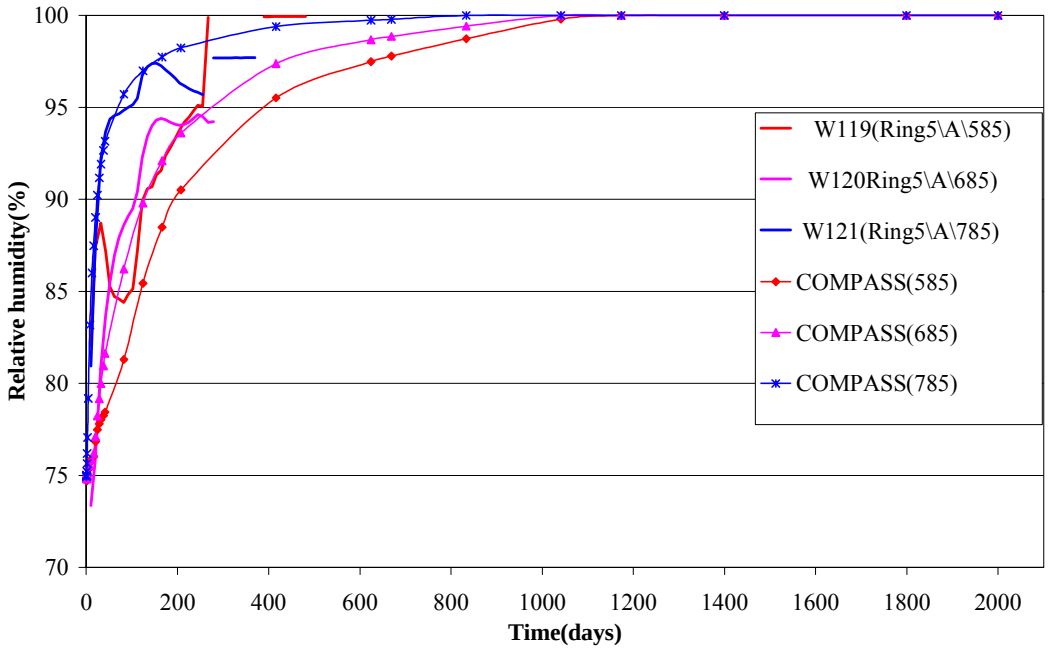

Figure 3.1.25: Relative humidity comparisons

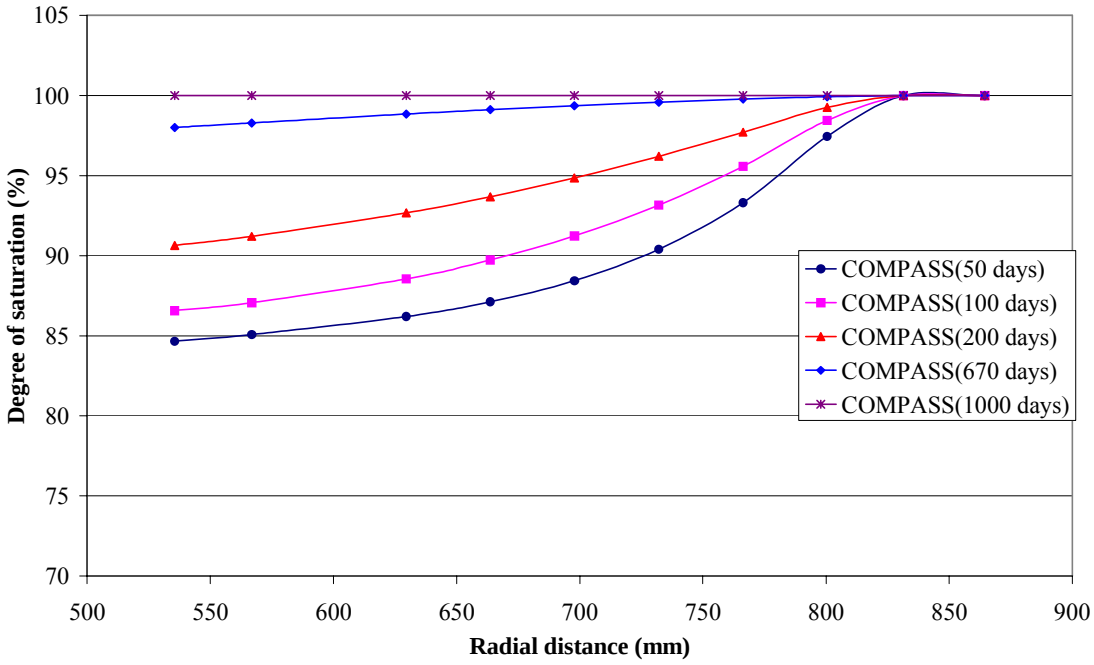

Figure 3.1.26: Computed profiles of degree of saturation

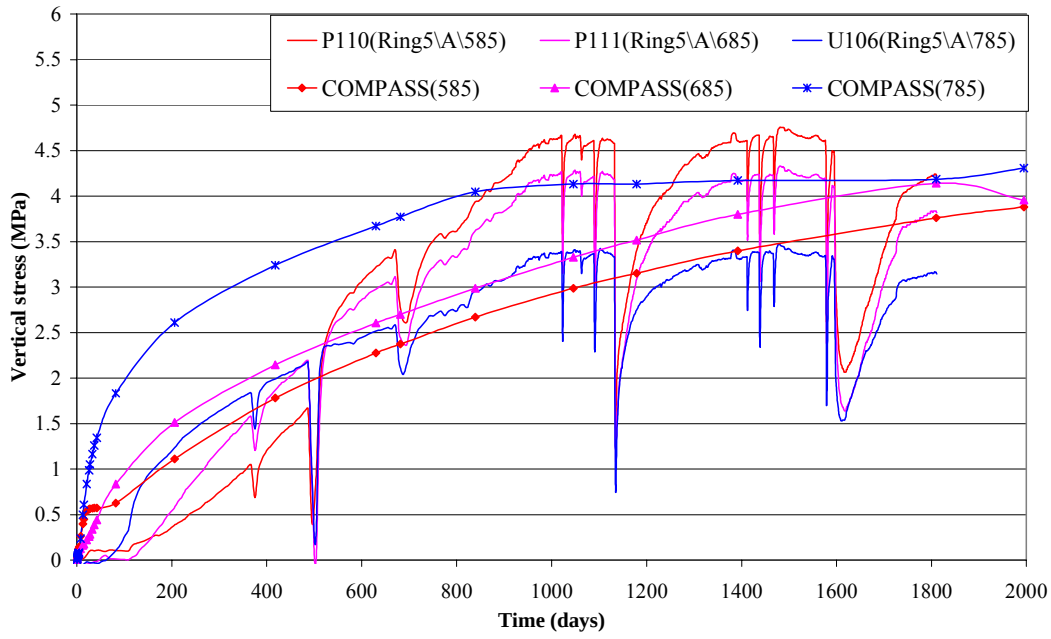

Figure 3.1.27 Vertical (axial) stress comparisons.

F. IRSN (CAST3M)

The CRT-1D has been modelled using axisymmetric two-dimensional finite elements. The interface between the canister and the bentonite has been treated by means of a special element. The overall mesh is displayed in Figure 3.1.28

Figure 3.1.28. Mesh used for the CRT-1D simulation.

In the interface element, as long as the gap is not closed, the presence of liquid water at atmospheric pressure is assumed (as they were some doubts about the initial hydraulic state of the interface) and a thermal exchange through this water layer is assumed between the canister and the bentonite. Once the gap is closed, the boundary is considered as impervious, the canister temperature is assigned to the bentonite boundary and a negative radial displacement is prevented. On the upper and lower surfaces of the model, the heat and flow fluxes, and the normal displacements are zero.

To improve the results of simulation, the effect of swelling was incorporated in the mechanical model. The comparisons between calculated and measured data are shown in Figures 3.1.29 to 3.1.31 and the final dry density of the buffer is plotted in Figure 3.1.32.

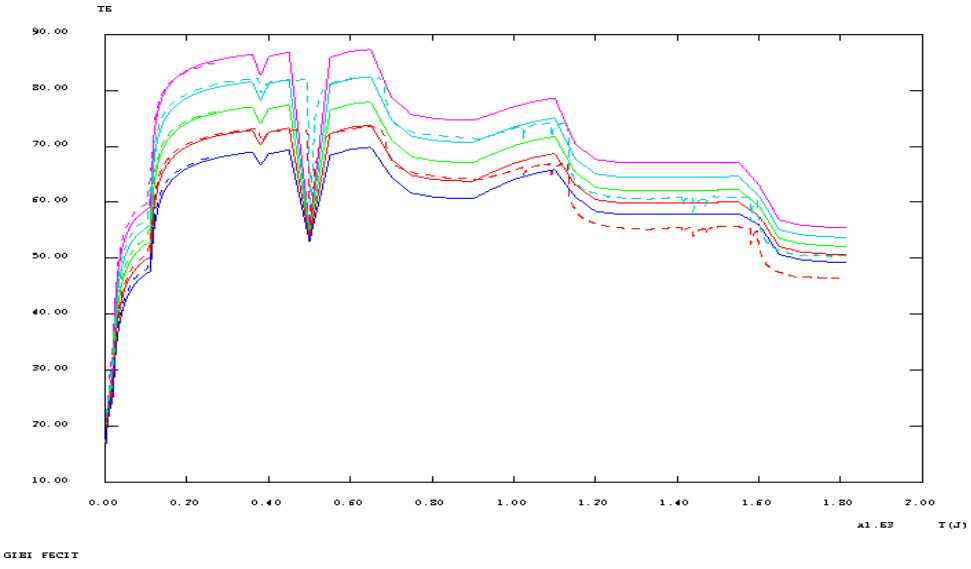

Figure 3.1.29. Comparison of temperature evolutions for the base case (dashed lines: measured values, full lines: computed values).

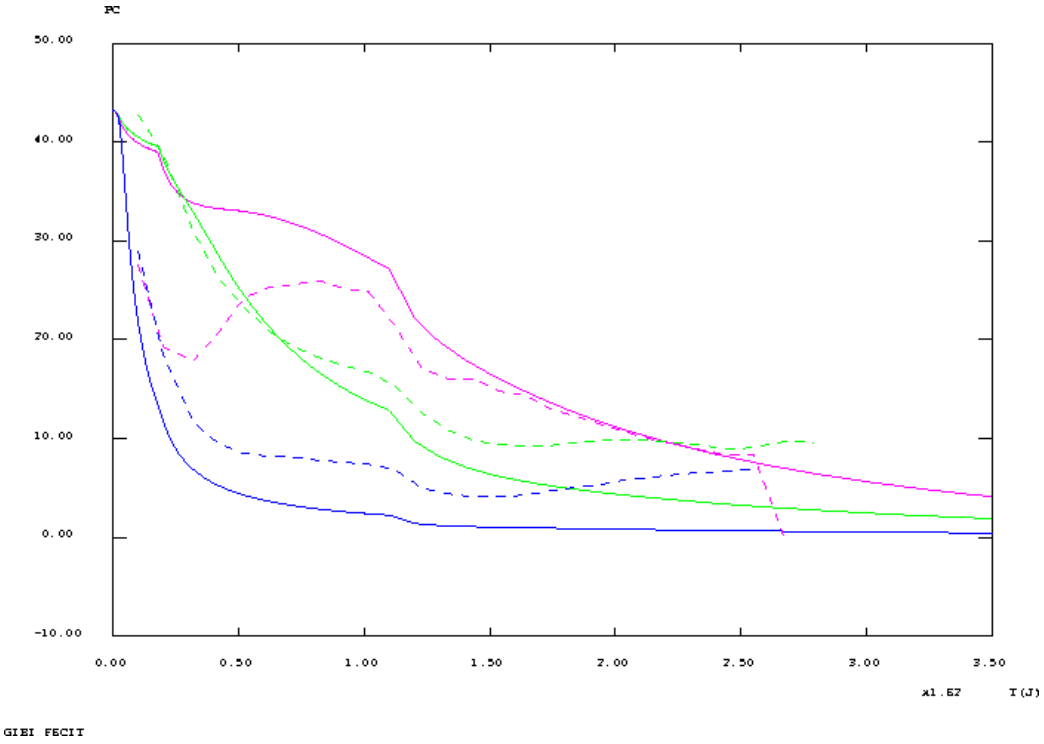

Figure 3.1.30. Comparison of short term capillary pressure evolutions for the new model (dashed lines: measured values, full lines: computed values).

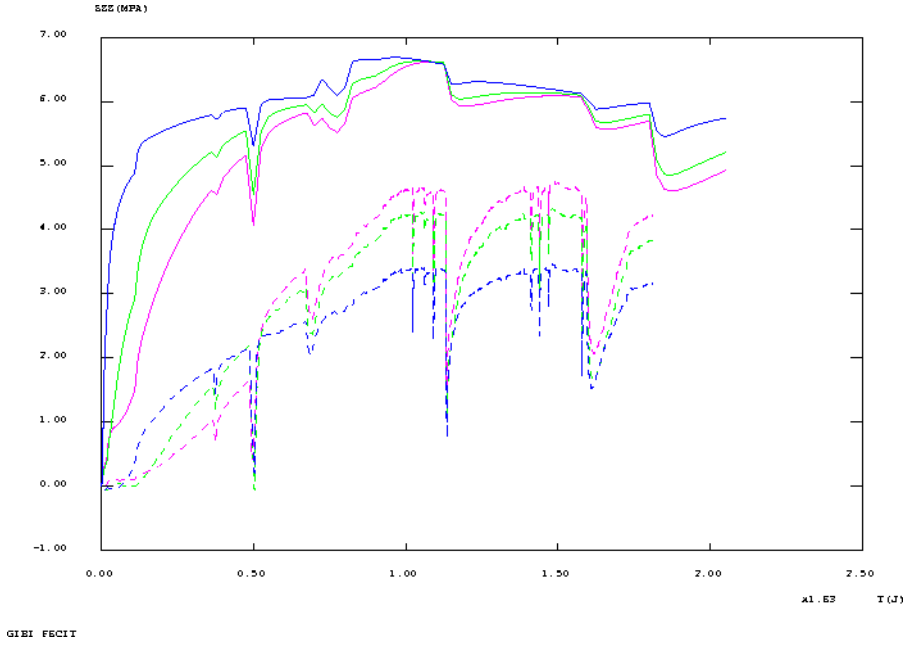

Figure 3.1.31. Comparison of vertical total stress evolutions for the new model (dashed lines : measured values, full lines : computed values).

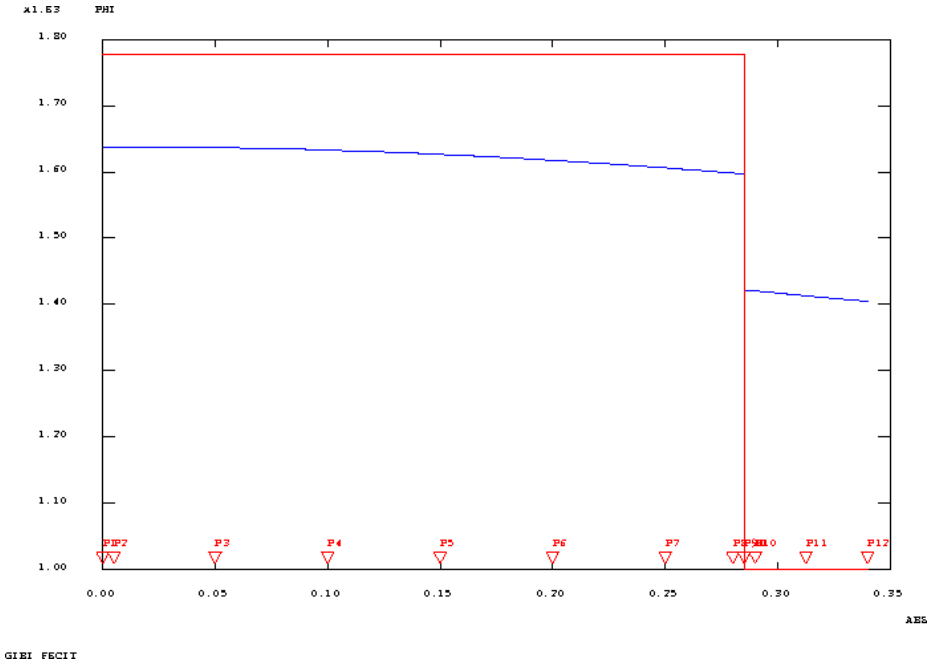

Figure 3.1.32: Comparison of bentonite dry density initial (red) and final (blue) profiles.

3.2 Thermo-hydro-mechanical simulation of the full Canister Retrieval Test

3.2.1 Description of the case

The geometry considered in this case is shown in Figure 2.1

Initial and Boundary conditions

The thermal load (canister power) can be obtained from the protocol given in Table 2. In Table 7 the rest of the boundary conditions are given whereas Table 8 contains the initial conditions.

Table 7: Boundary conditions

Type of process		
Thermal	Hydraulic	Mechanical
Tunnel air temperature T=15 ºC	Water pressure from filter protocol.	The effect from the rock anchors should be modelled. The steel lid and concrete plug are allowed to move in the vertical direction.

Table 8: Initial conditions.

	Type of process		
Constituent	Thermal	Hydraulic	Mechanical
Bentonite blocks -Cylinder-shape -Ring-shape	 T=20 ºC T=20 ºC	 S_r=0.751 S_r=0.859	 s=0MPa, n=0.39 s=0MPa, n=0.36
Pellet-filled gap	T=20 ºC	S_r=0.895	s=0MPa, n=0.64
Bentonite bricks	T=20 ºC	S_r=0.637	s=0MPa, n=0.42

Results requested

For Ring 5 (at canister mid-height, 2.84 m from the borehole bottom) all the results specified for the previous task should also be presented for this task, where the entire buffer is considered. In addition, the history of variables belonging to points in Ring 10 (at the top of the canister, 5.34 m from the borehole bottom) and Cylinder 3 (the second ring from the top, 6.25 m from the borehole bottom) should also be provided.

Steady state

It was also proposed to continue with the simulation to reach the steady state of the buffer applying the following boundary conditions:

- Heater power held constant to 1150W after day 1596 (March 10, 2005)
- Water pressure held constant and equal to 0 after day 1598 (March 12, 2005)

When steady state conditions are reached the following parameters should be reported:

- Saturation time of the bentonite buffer (in the cylinder and ring zones)
- Radial and axial stresses in the bentonite buffer
- Average and distribution of dry density (porosity)
- Average and distribution of permeability (or hydraulic conductivity)

3.2.2 Results obtained by the modelling groups

A. CIMNE (Code_Brigth)

The geometry used for simulation is axisymmetric and it included eight materials (Figure 3.2.1). The materials are: bentonite cylinders, rings and bricks, pellets, gap, canister, concrete plug and steel lid. The geometry is discretized by 4-noded quadrilateral structured elements, and the mesh includes 1449 elements and 1540 nodes.

The energy flux along the boundary (pellets-rock boundary) was calibrated using a reference temperature of 20ºC, and different values of the spring constant, g (Figure 3.2.1). The calibration of g values was performed to obtain temperature results similar to those measured by the sensors located at the rock. The effect of the anchors was considered as a point force applied on the centre of the steel lid. The simulation of the test was extended up to 2700 days with the objective of reaching the steady state situation of the test.

The comparison between calculated and measured temperatures is shown in Figure 3.2.2. The relative humidities are plotted in Figures 3.2.3 to 3.2.5. The evolution of vertical stress is shown in Figure 3.2.6. The final degree of saturation of the buffer is given in Figure 3.2.7 and the dry density in Figure 3.2.8. And the evolution of the plug displacements is given in Figure 3.2.9.

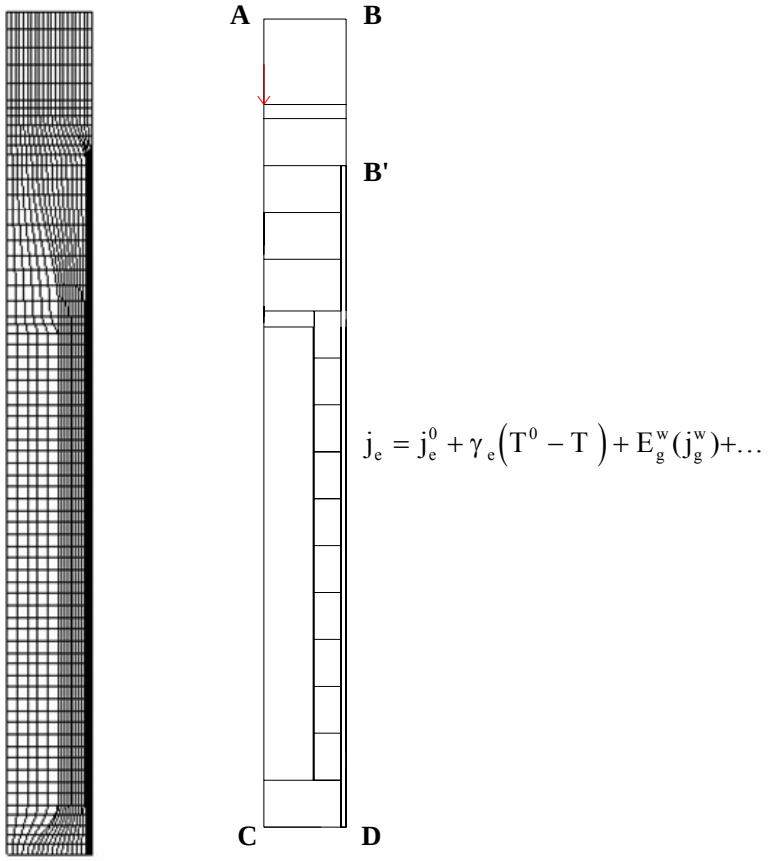

Figure 3.2.1. Geometry and mesh of the test.

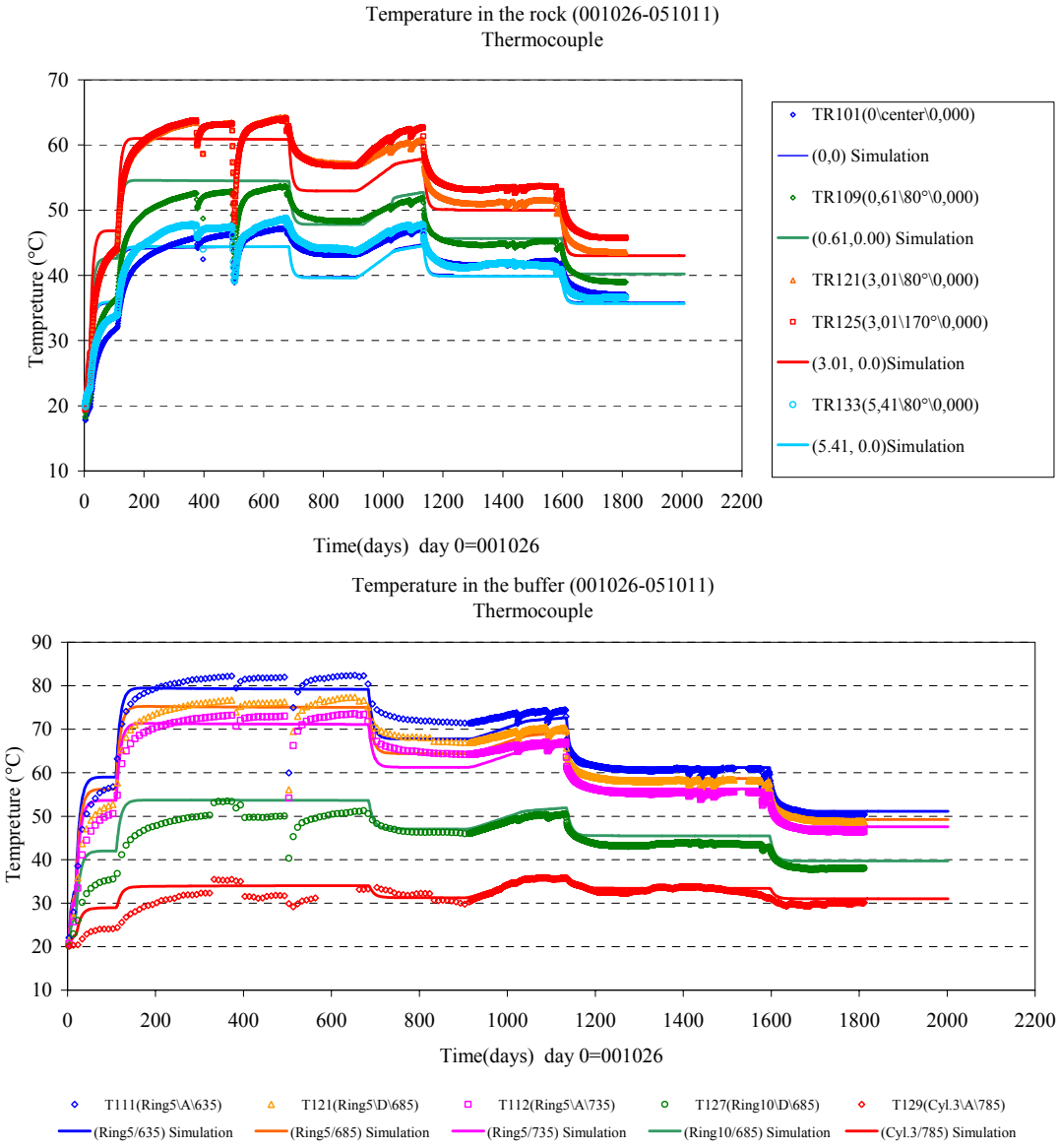

Figure 3.2.2 Temperature evolution in the rock (upper graph-indicated as red dots in the plot) and in the buffer (lower graph-indicated as blue dots in the plot).

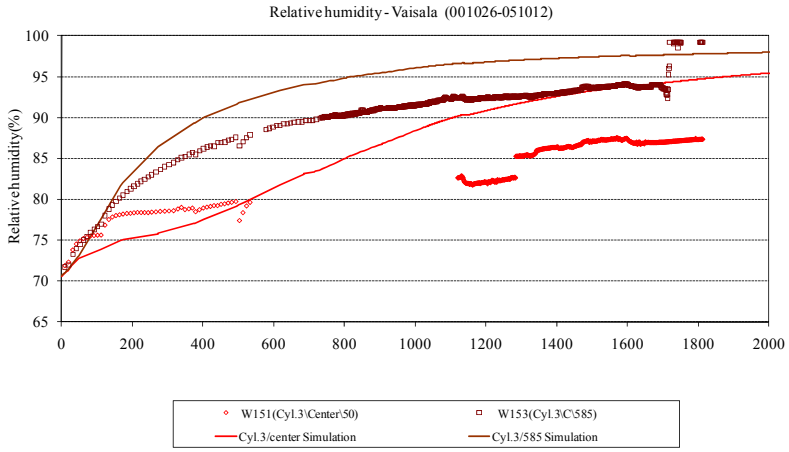

Figure 3.2.3: Comparison of measured and calculated relative humidity for Cylinder 3.

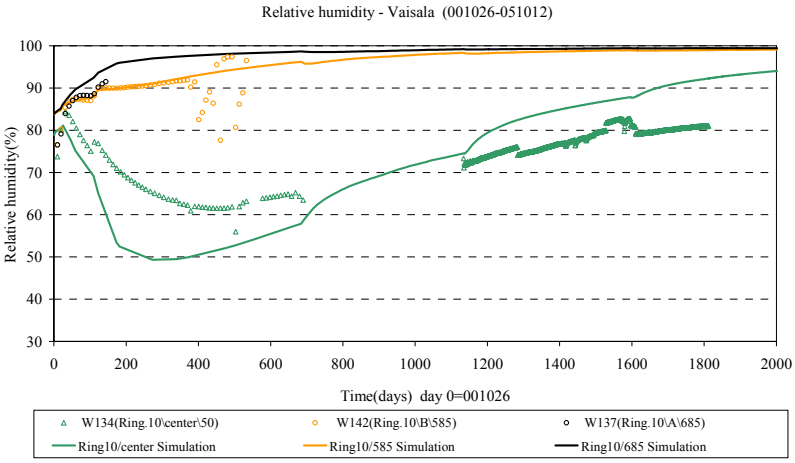

Figure3.2.4: Comparison of measured and calculated relative humidity for Ring 10.

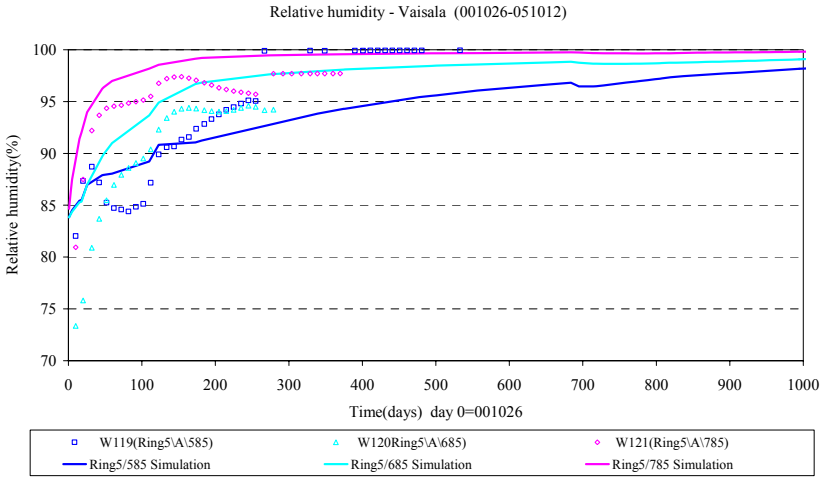

Figure3.2.5: Comparison of measured and calculated relative humidity for Ring 5

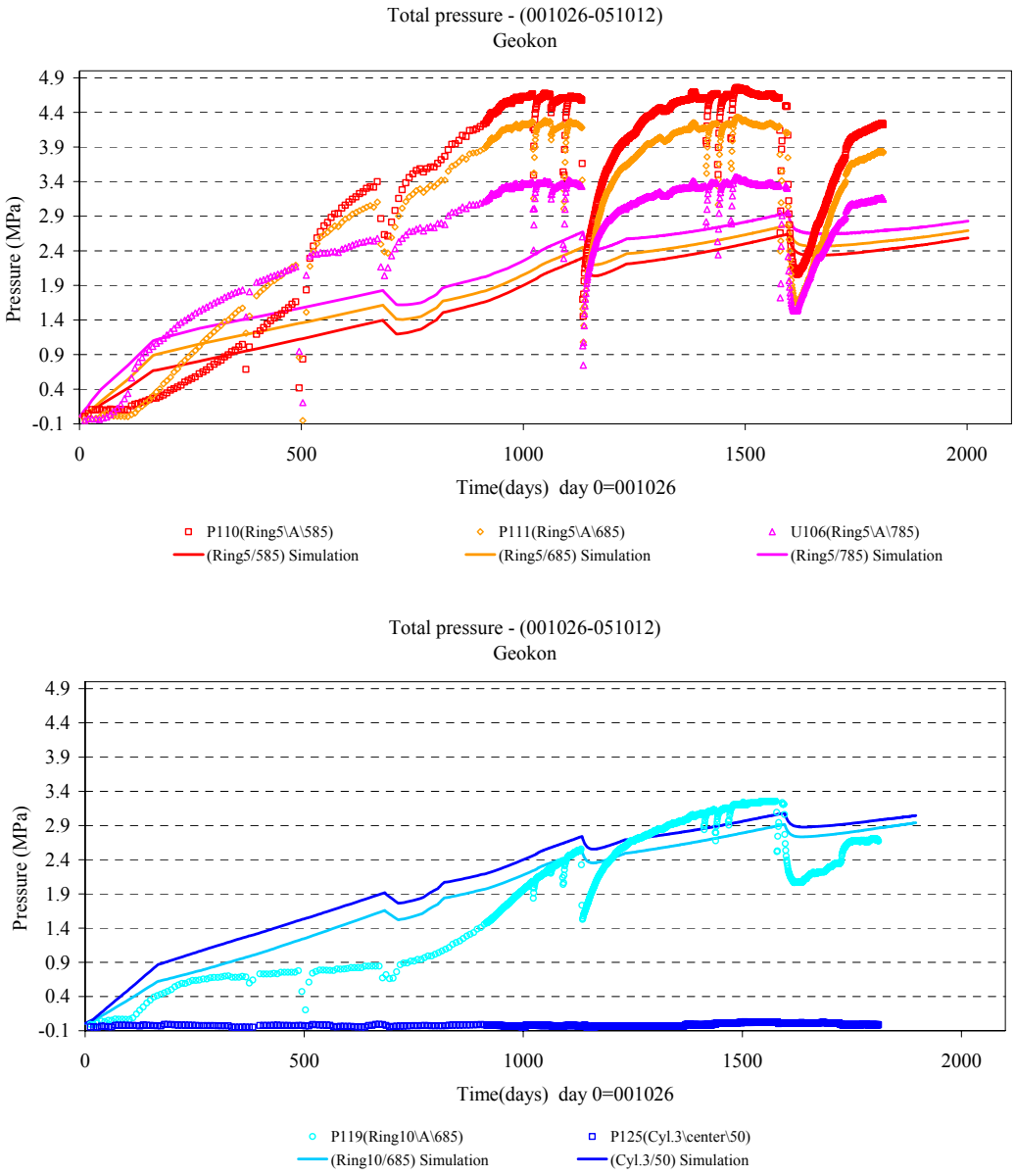

Figure 3.2.6: Comparison of total pressure evolution, measured and calculated.

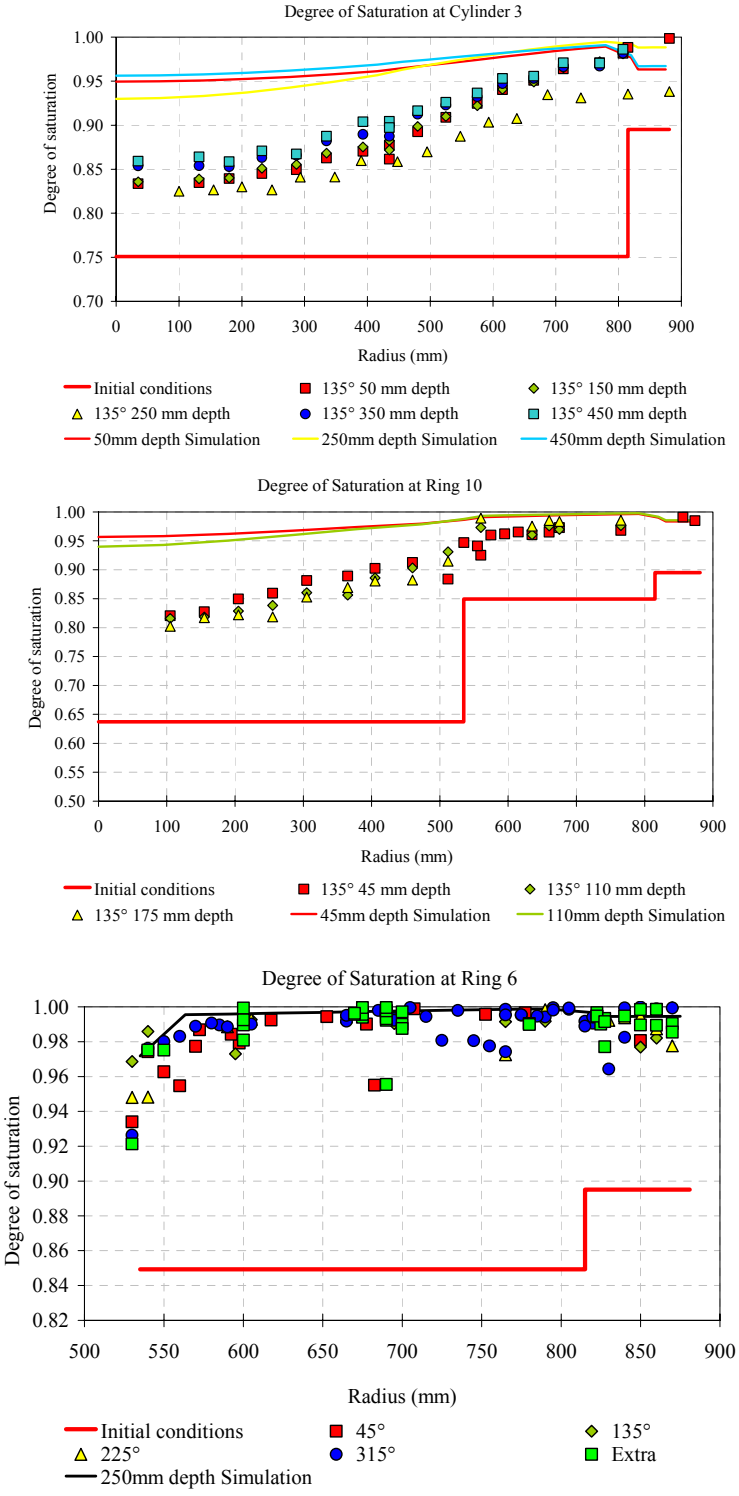

Figure3.2.7: Final degree of saturation for Cylinder 3, Ring 10 and Ring 6.

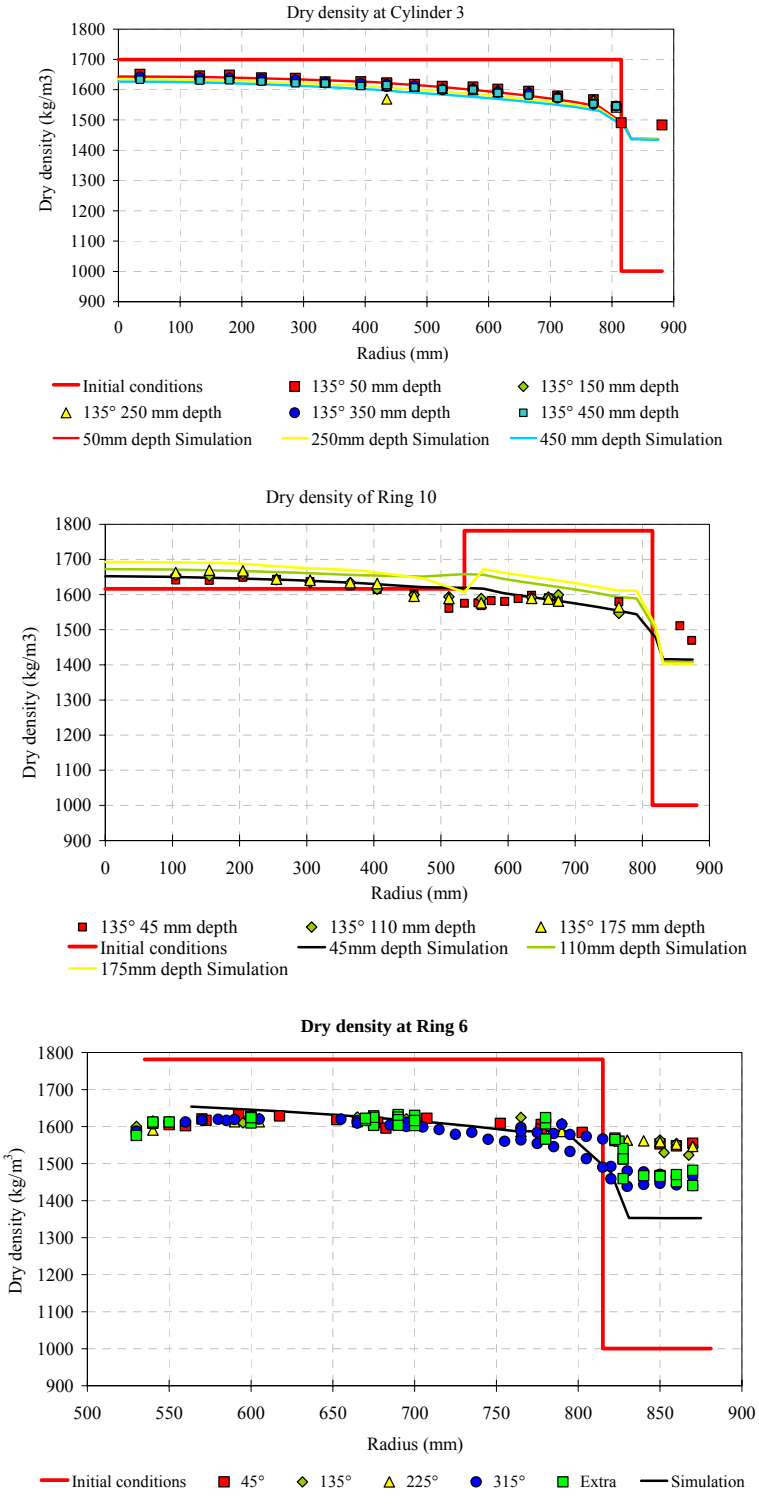

Figure3.2.8: Final dry density for Cylinder 3, Ring 10, Ring 6

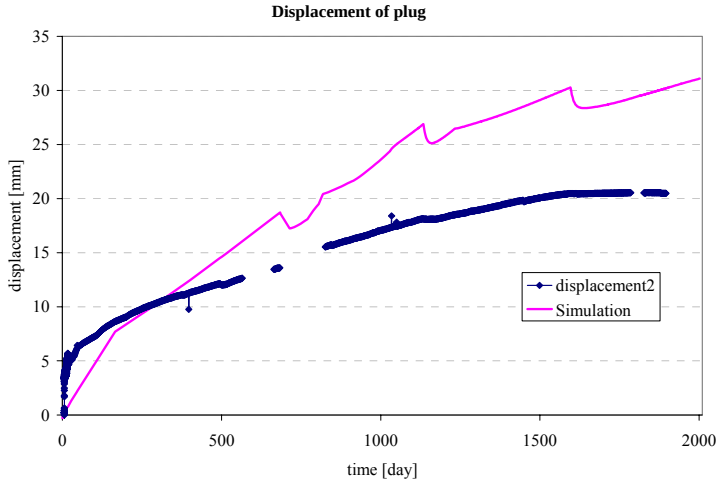

Figure 3.2.9: Comparison between plug displacements, measured and computed.

The simulation of the test was extended up to 2700 days with the objective of reaching a steady state situation of the test. In this period it was observed that the stresses of the buffer continued increasing but at a very small rate, and show a tendency to be constant. Something similar occurs with dry densities and degrees of saturation.

B. Posiva/Marintel (FreeFemm++)

The simulation mesh used is shown in Figure 3.2.10. It consists of 982 triangular elements. Time step was fixed to 5 days.

Figure 3.2.10: FEM mesh used in simulation of CRT

The pellet-filled gap was simulated as an elastic boundary condition such that twice the swelling pressure was required to compress the filling to dry density of the initial

buffer material. This resulted to spring constant 2.38×108 Pa m^{-1}. This is equivalent to use a single element layer (justified by assuming homogeneity) with initial full saturation (justified by quick saturation shown by measurements) and with linear mechanical behaviour (also used for the compacted material).

The comparison of relative humidities for Cylinder 3 and Ring 10 are plotted in Figure 3.2.11 and in Figure 3.2.12 for Ring 5. Total pressure for Ring 5 is shown in Figure 3.2.13. And the displacement of the plug is given in Figure 3.2.14.

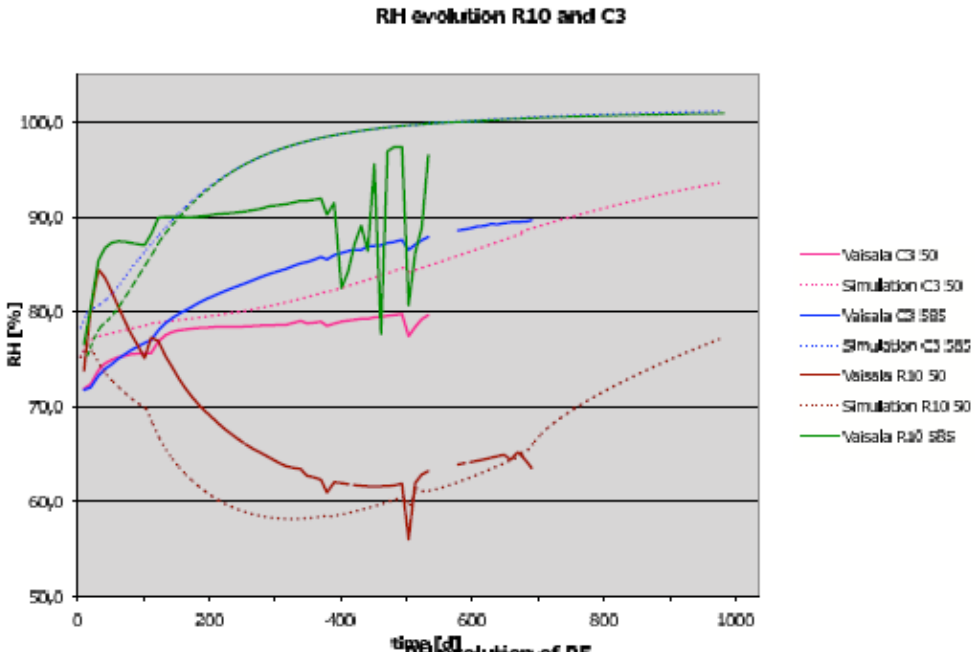

Figure 3.2.11: Simulated RH for Cylinder 3 and Ring 10.

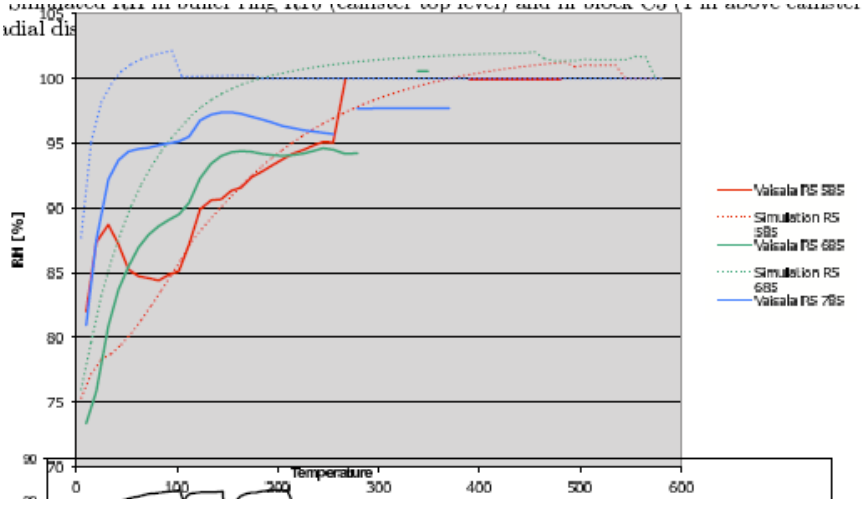

Figure 3.2.12. Simulated RH for Ring 5.

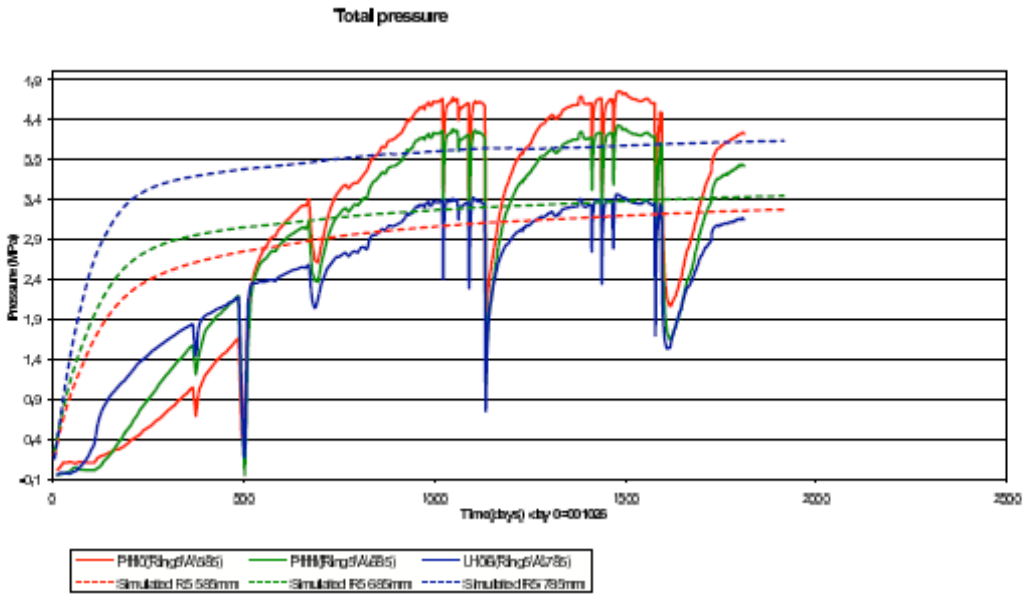

Figure 3.2.13: Total pressure for Ring 5.

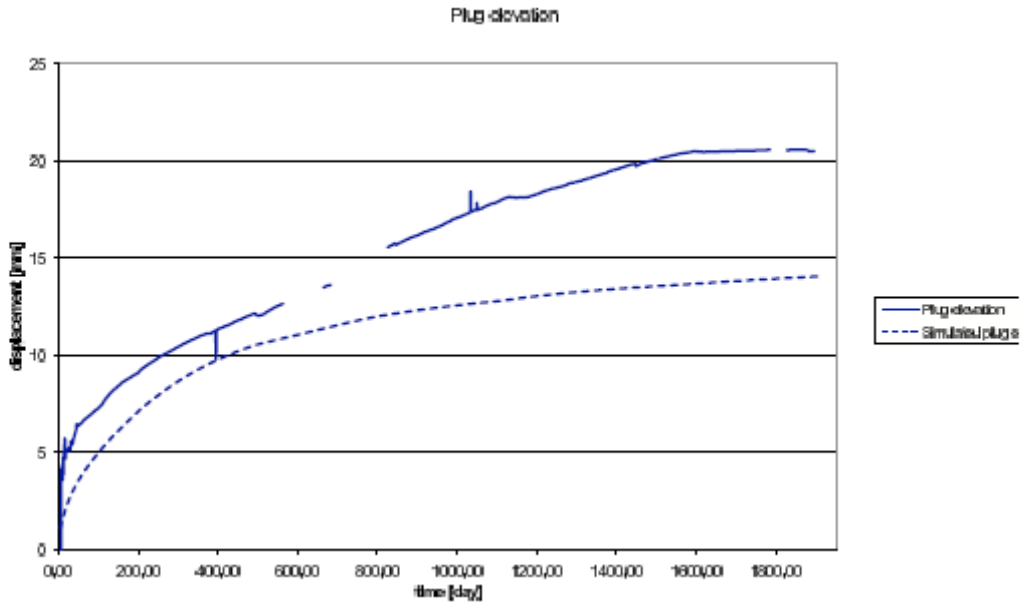

Figure 3.2.14: Displacement of the plug.

Steady state: The experiment was not fully saturated at the end of the test, nor it had reached stationary state. To achieve steady state conditions, the simulation was continued to t = 30 years. Stationary state for water inflow is reached approximately at t = 20 years. Full saturation is reached already at t ≈ 13 years, but water flow continues after that because water pressure is not yet in equilibrium with the boundary pressure of 0.85 MPa.

C. KTH (ROLG)

The model geometry has a cylindrical shape, with diameter and height equal to 7m and 10m, respectively. Hexahedron elements are used to build the 3D FEM mesh Figure 3.2.12. The number of nodes is 10620. The number of elements is 11130.

The evolution of temperatures are given in Figure 3.2.16 for ring 10 and Figure 3.2.17 for Cylinder 3. Relative humidities are plotted in Figure 3.2.18. The vertical stress is shown in Figures 3.2.19 and 3.2.20. The final degree of saturation of the buffer is plotted in Figure 3.2.21 and the final dry density is given in Figure 3.2.22. Finally, the plug displacements are shown in Figure 3.2.23.

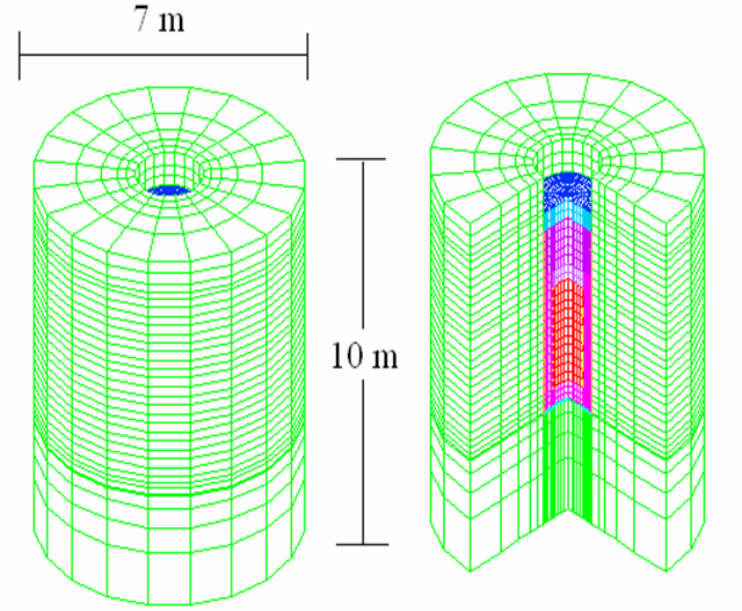

Figure 3.2.15: 3-D FEM mesh for the full scale 3D CRT model

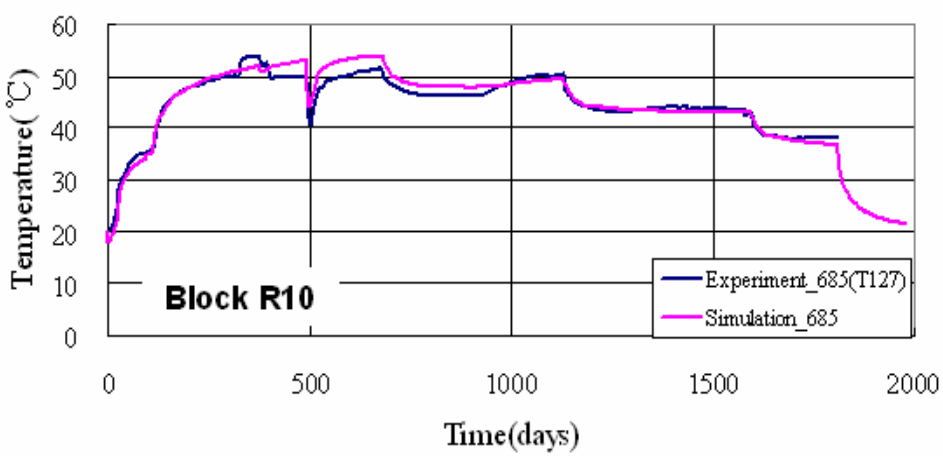

Figure 3.2.16 Comparison between the simulated and measured temperatures in Block R10

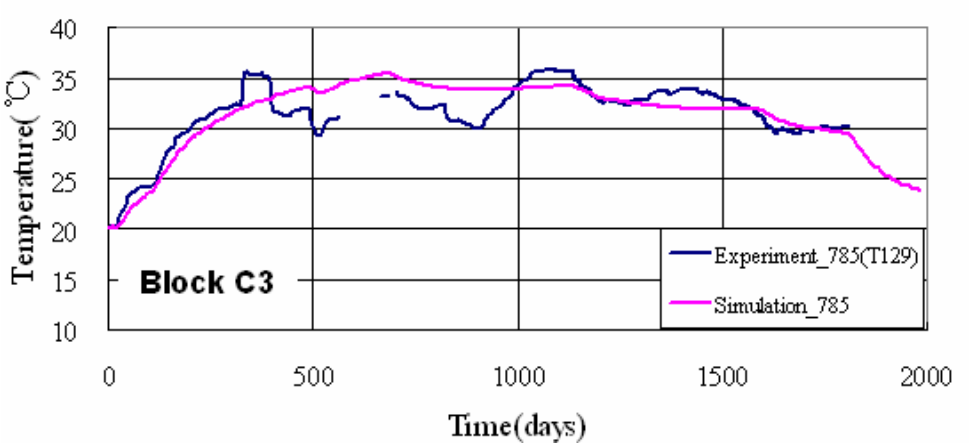

Figure 3.2.17: Comparison between the simulated and measured temperatures in Block C3.

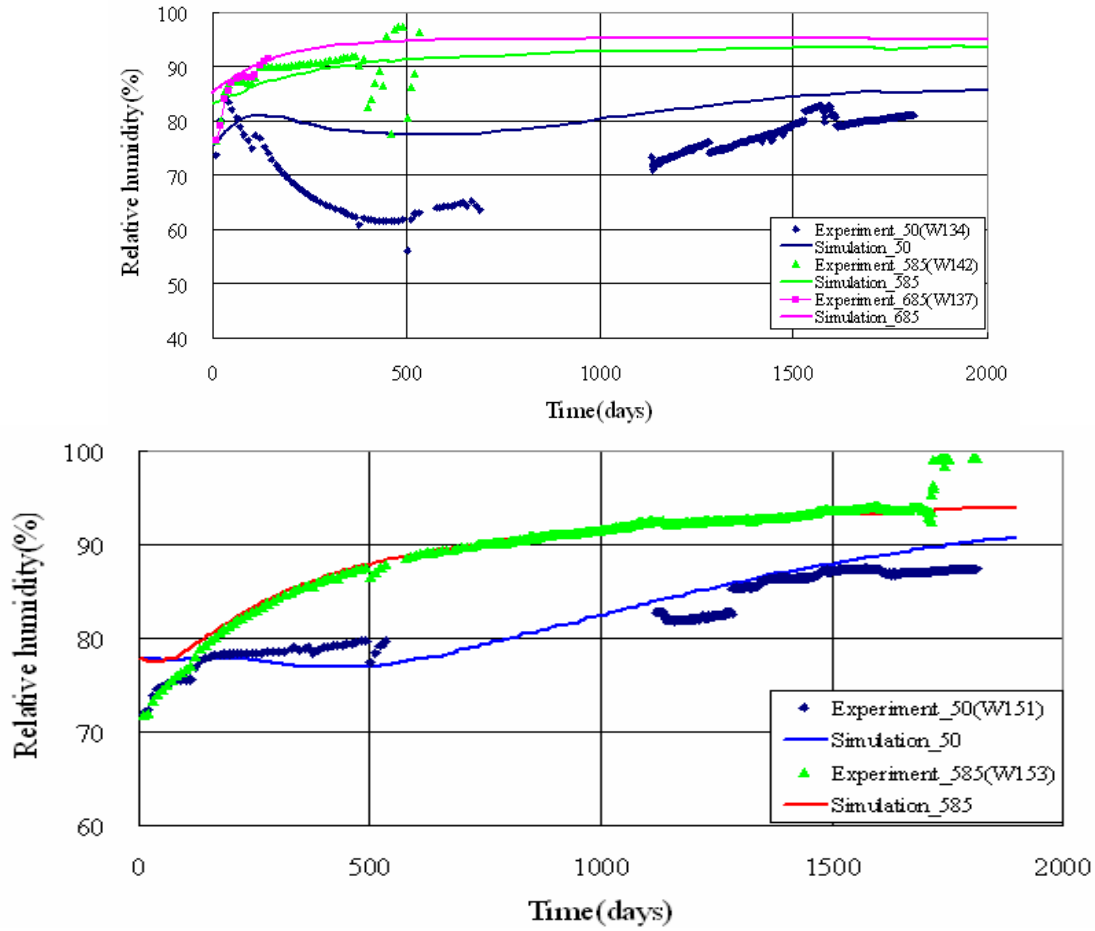

Figure 3.2.18: Measured and simulated relative humidity of Block R10 (top) and of Block C3 (bottom)

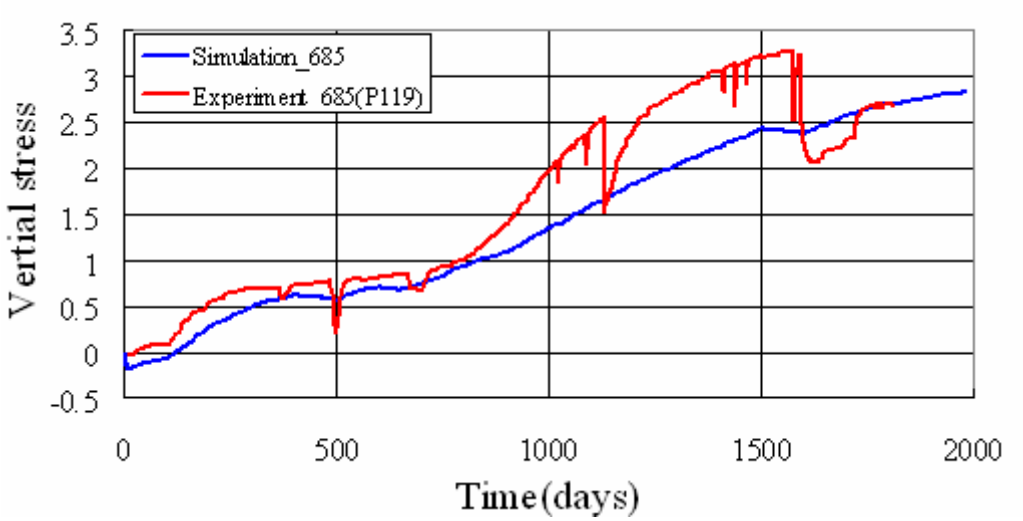

Figure 3.2.19: Measured and simulated vertical stress evolutions of Block R10

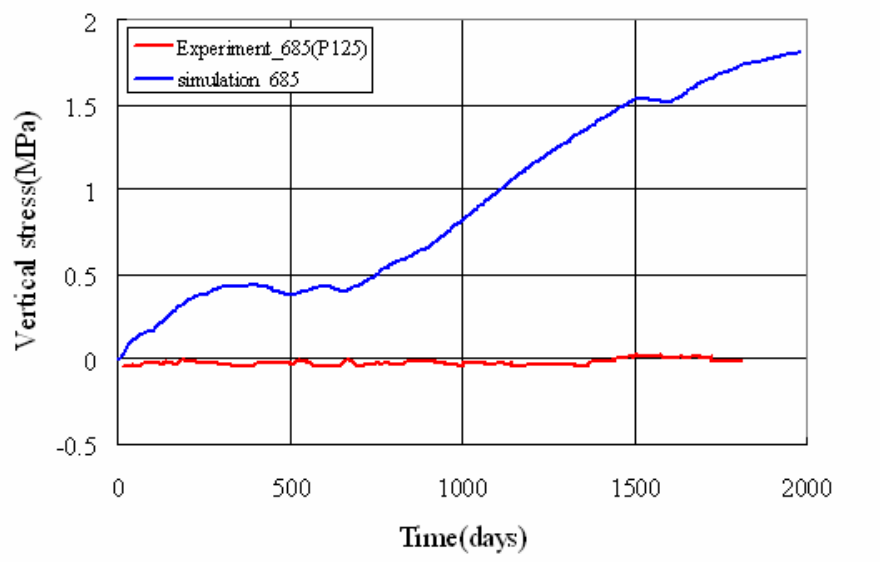

Figure 3.2.20 Comparison between simulated and measured vertical stress in Block C3.

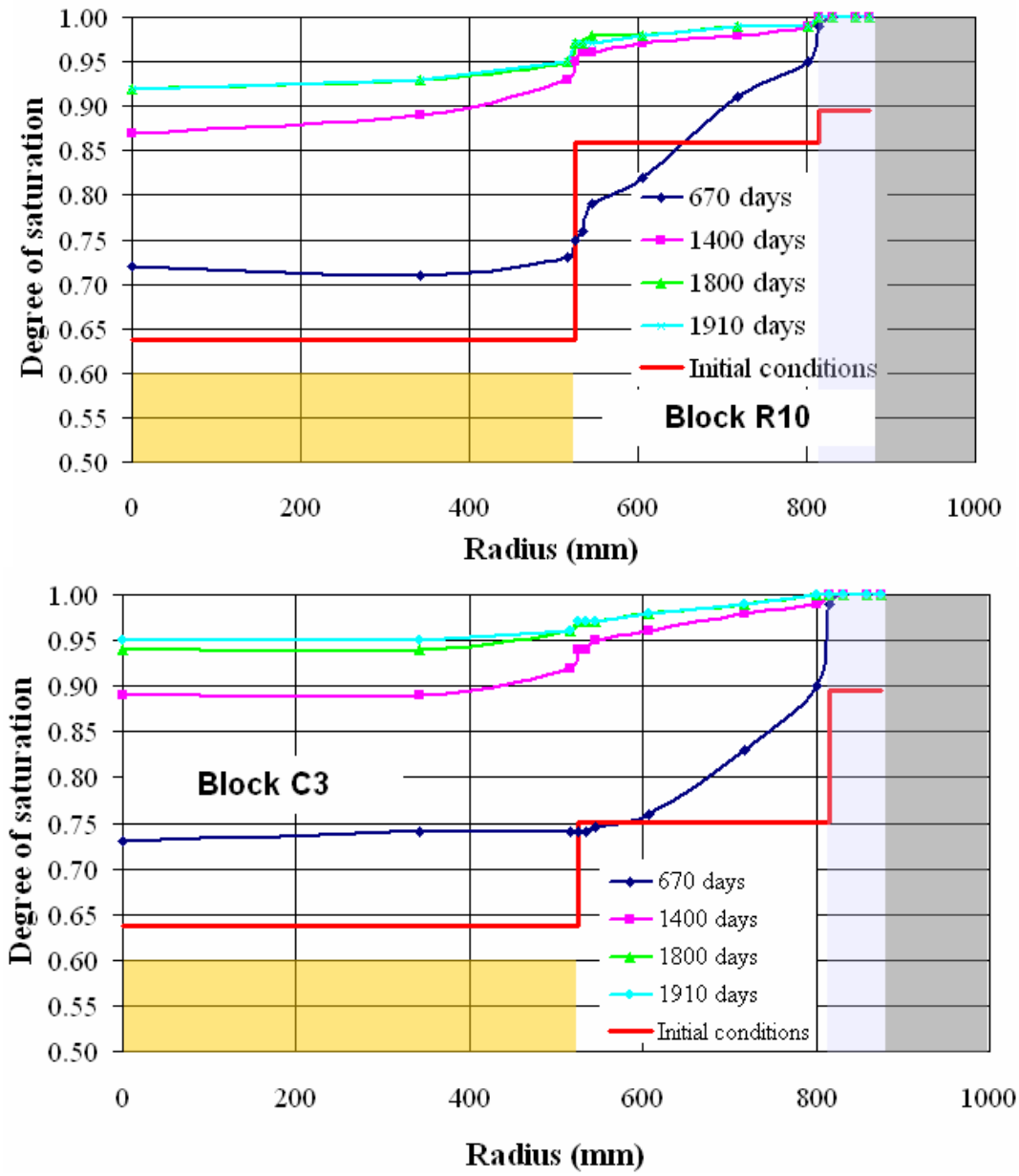

Figure 3.2.21: Simulated profiles of degree of saturation of Ring10 and Cylinder 3 at different times.

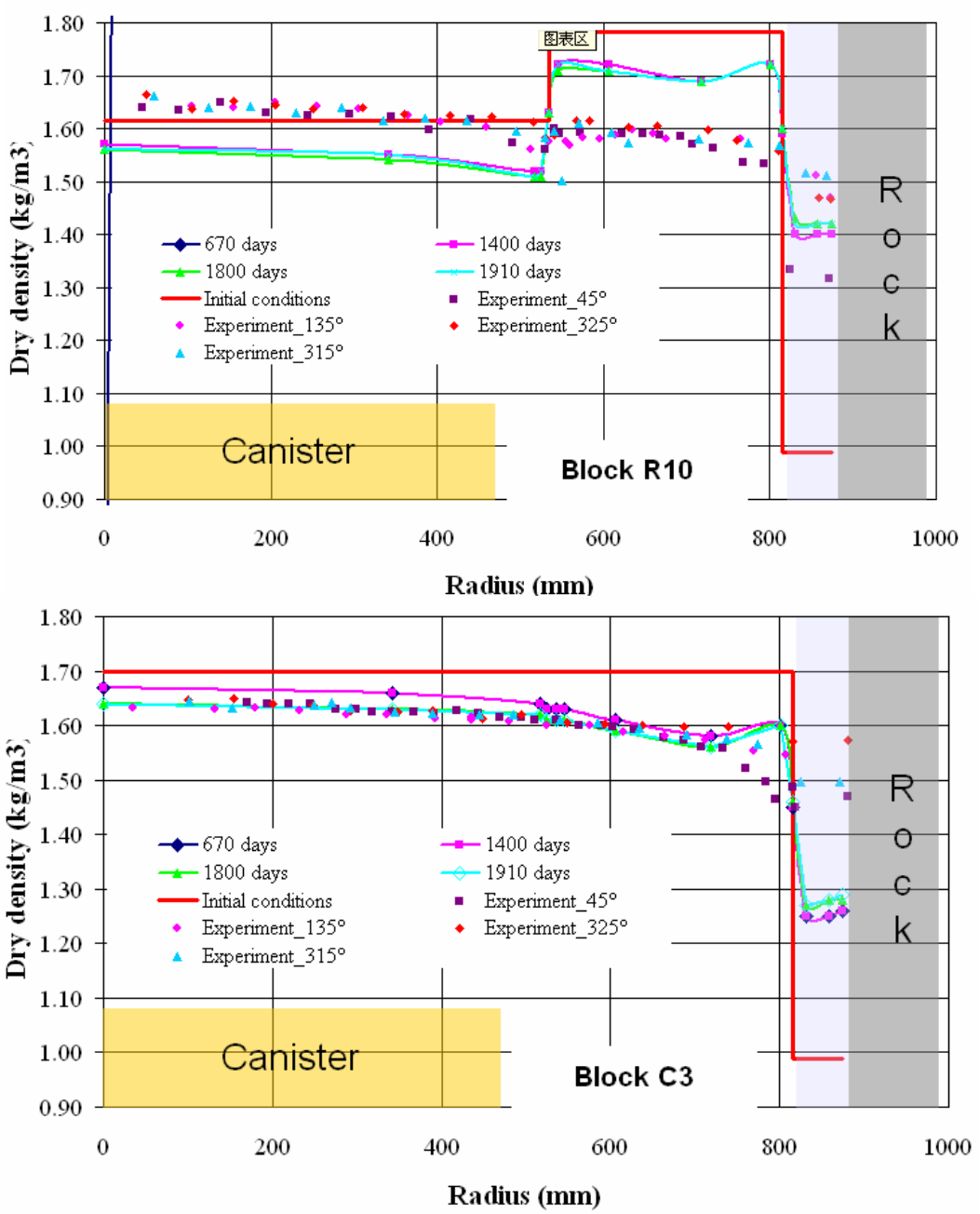

Figure 3.2.22: Measured and simulated profiles of dry density profiles of Ring 10 and Cylinder 3 at different times.

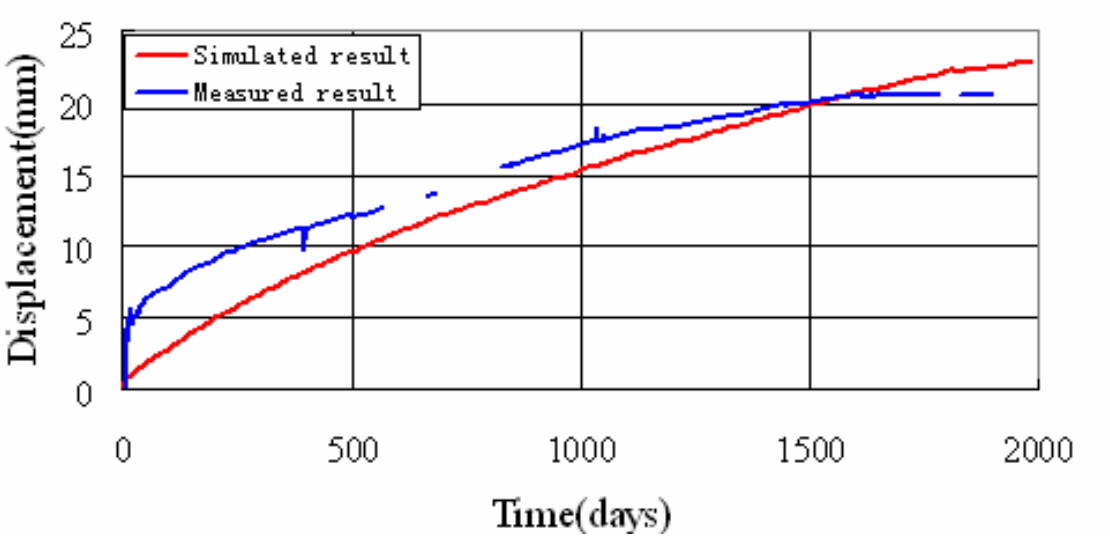

Figure 3.2.23. Measured and simulated evolutions of the plug displacement

Steady state:

The following average parameters were calculated at steady state after an analysis taken to 13000 days (about 35 years).

Bentonite	Ring shape	Cylinder shape	Bricks	Pellets	Whole buffer
Average saturation	0.998812	0.999366	0.999511	0.999076	0.999118
Average radial stress(MPa)	0.831	2.869	3.360	0.945	1.854
Average axial stress(MPa)	1.334	3.857	4.962	1.864	2.661
Average dry density (g/cm^3)	1.675	1.567	1.479	1.526	1.602
Average permeability (m^2)	1.015×10^{-21}	2.74×10^{-21}	5.097×10^{-21}	3.954×10^{-21}	2.28×10^{-21}

D. Quintessa (QPAC-EBS).

The geometry, materials and compartments used in the simulation are shown in Figure 3.2.24.

The comparison between calculated and measured of Relative Humidity is shown in Figure 3.2.25. The radial stress of Ring 5 is plotted in Figure 3.2.26. The dry density at the end of the test for the buffer is shown in Figure 3.2.27. And the plug displacements is given in Figure 3.2.28.

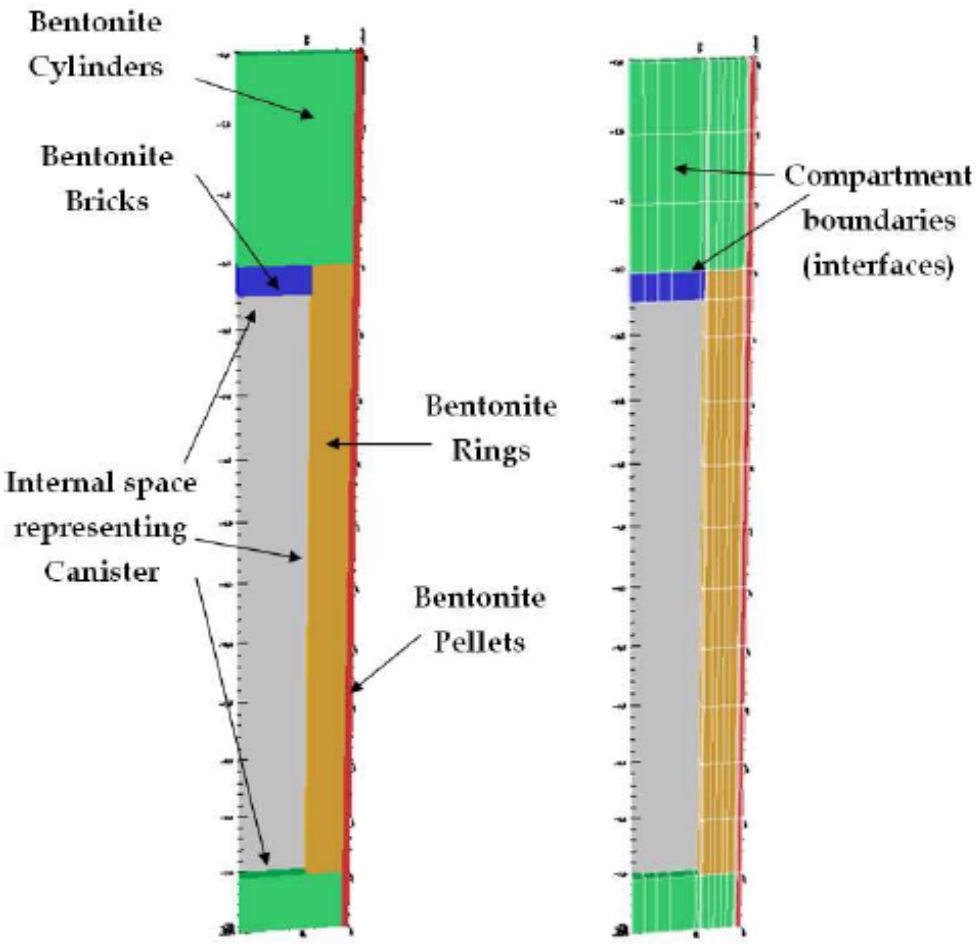

Figure 3.2.24: System Discretisation

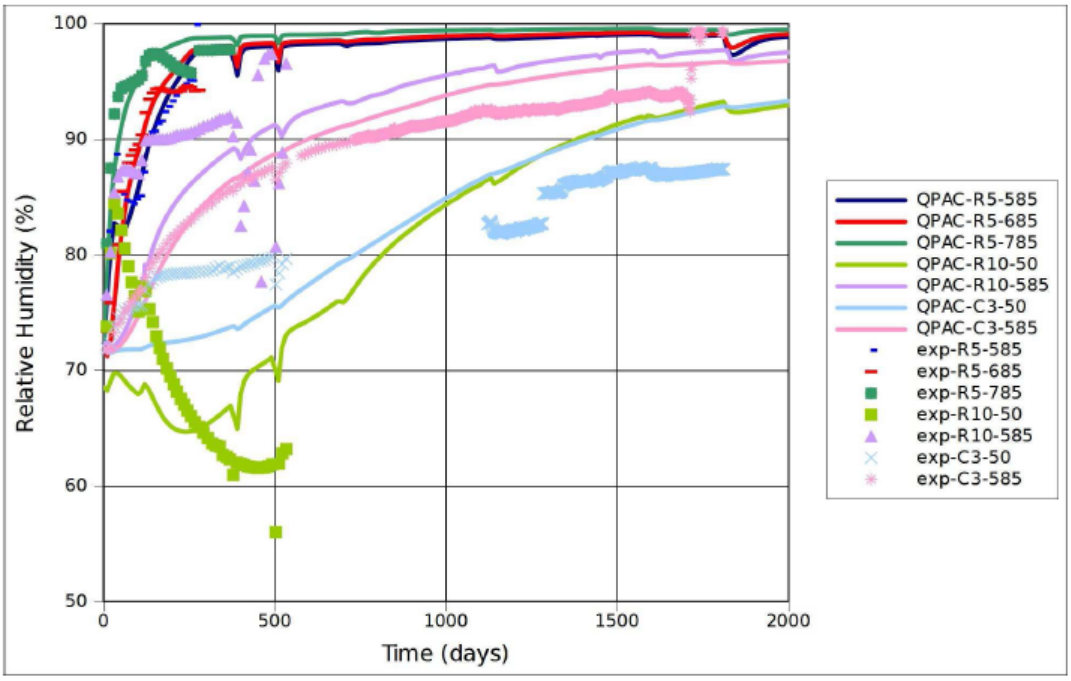

Figure 3.2.25: Calculated and Measured Evolution of Relative Humidity

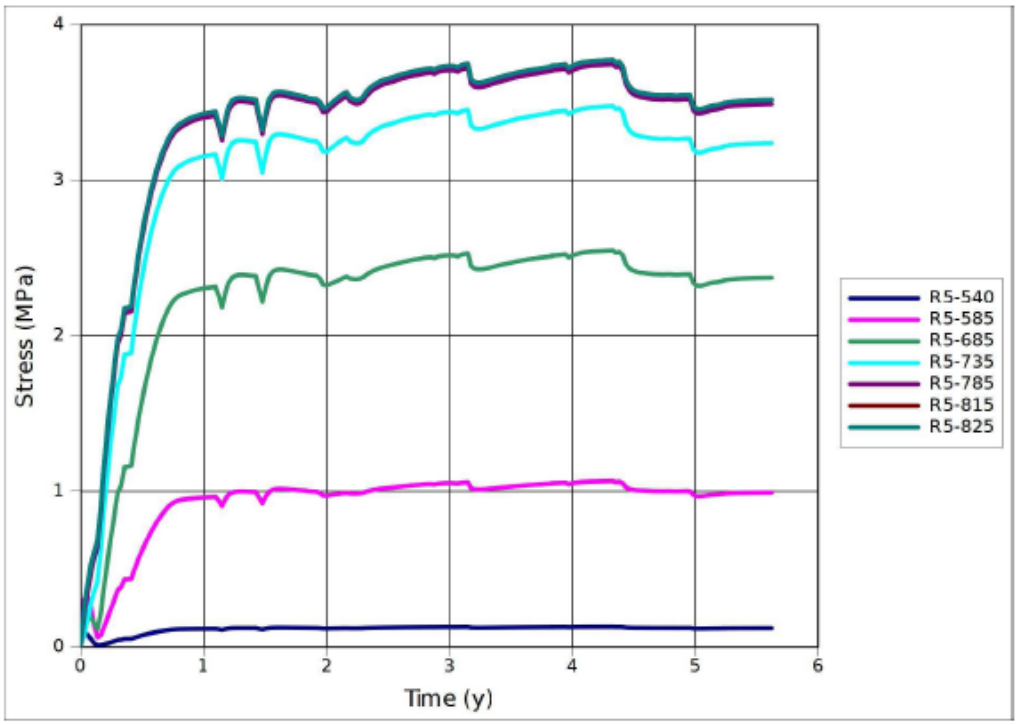

Figure 3.2.26: Calculated Evolution of Radial Stresses in Ring 5

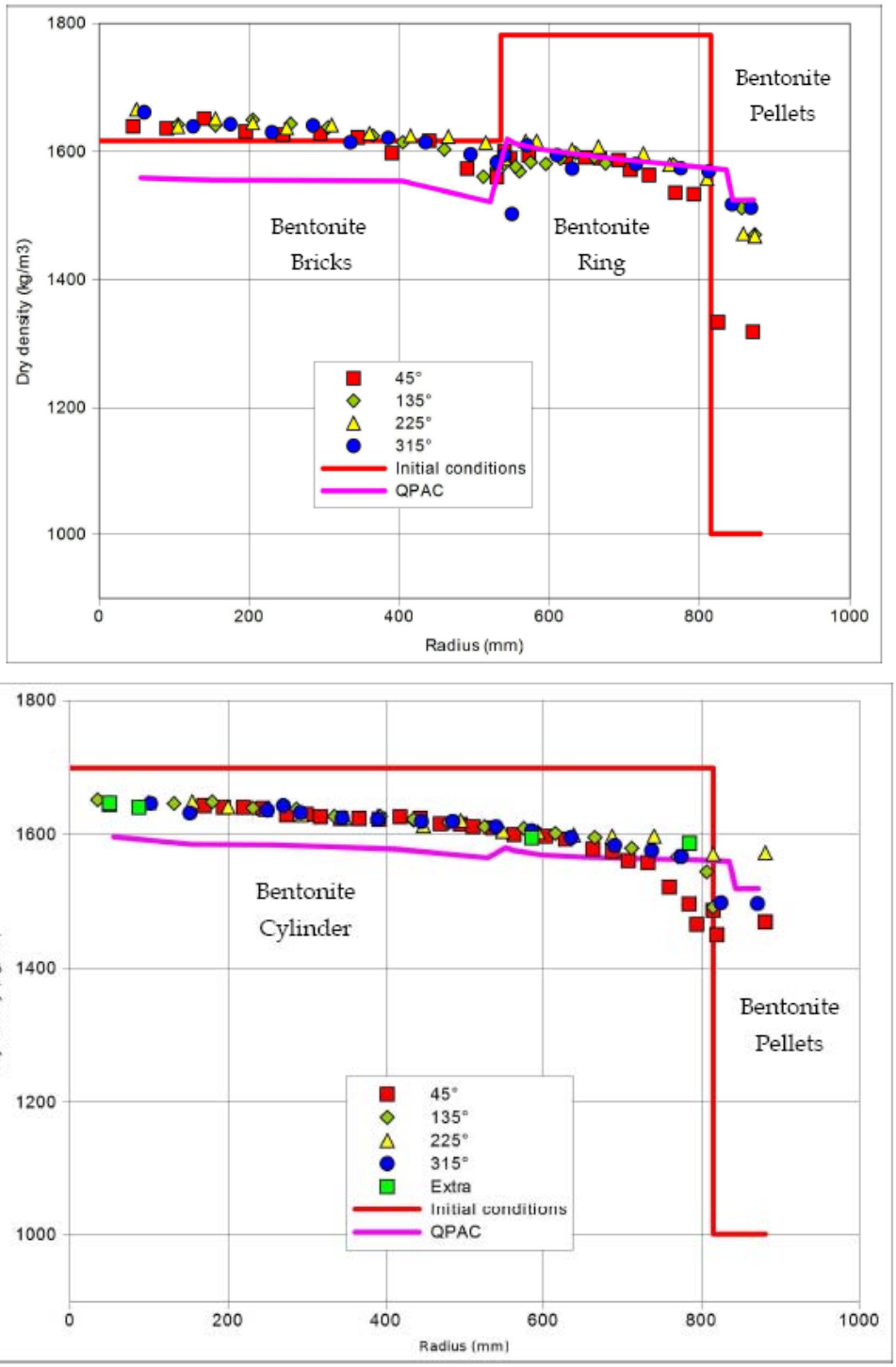

Figure 3.2.27: Comparisons between calculated and measured dry densities at the end of the experiment for Ring 10 (top) and Cylinder 3 (bottom)

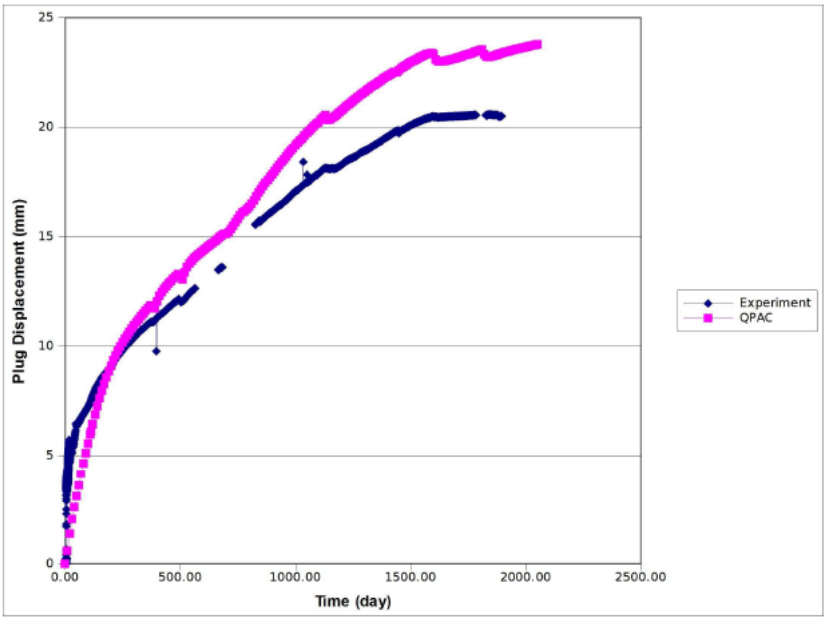

Figure 3.2.28: Calculated and measured plug displacements

Steady state:

The QPAC-EBS case was run for a total of 1000000 days (approximately 2738 years). The evolution of water saturation, dry density and intrinsic permeability are shown in Figures 3.2.29, 3.2.30 and 3.2.31.

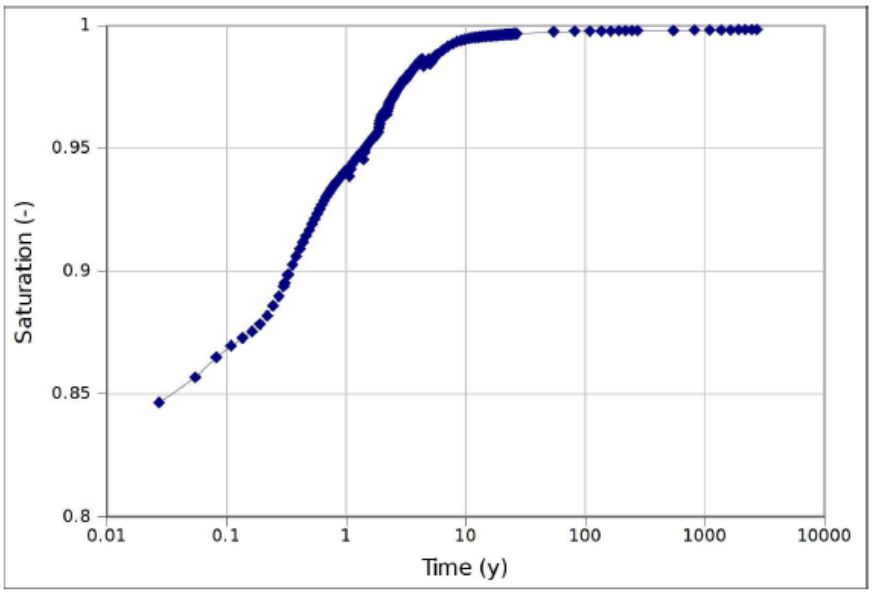

Figure 3.2.29: Calculated Average Water Saturation in the Bentonite

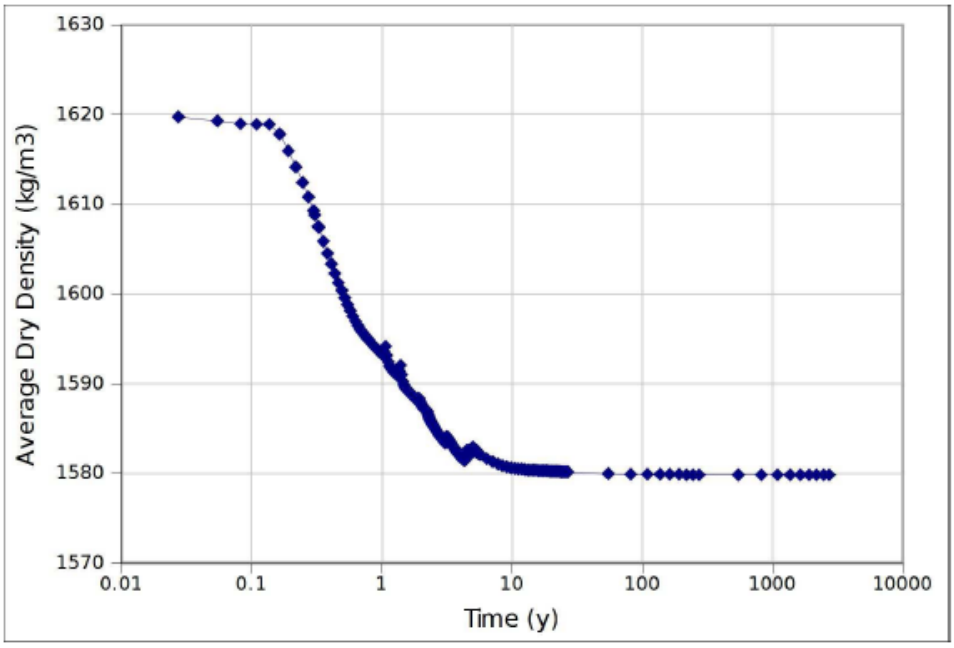

Figure 3.2.30: Calculated Average Dry Density in the Bentonite

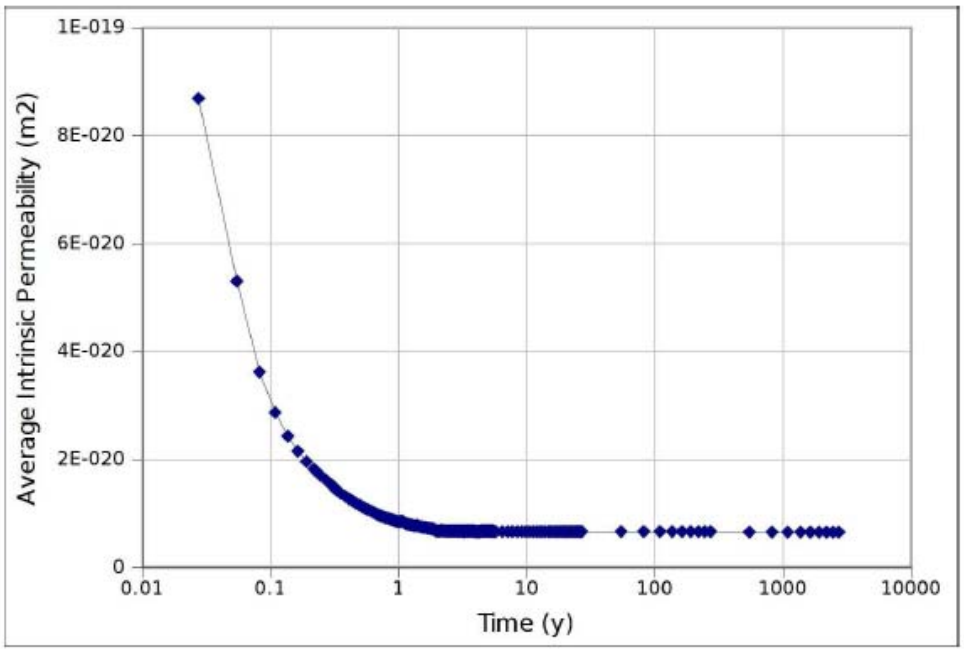

Figure 3.2.31: Calculated Average Intrinsic Bentonite Permeability

E. CU (COMPASS)

A 2D axisymmetric domain was used for the numerical analysis. A mesh consisting of 3712 three-noded isoparametric triangle elements was used. The calculation domain as well as the mesh, initial conditions and boundary conditions are shown in Figure 3.2.32. An initial time-step of 1000 seconds, being allowed to increase to a maximum of 1 day depending upon convergence criteria, was found to yield converged results.

The evolutions of temperature for Ring 5, Ring 10 and Cylinder 3 are plotted in Figures 3.2.33, 3.2.34 and 3.2.35 respectively. The comparison of relative humidity is shown in Figure 3.2.36 to 3.2.37. The comparison of vertical stress is plotted in Figure 3.2.38 for Ring 5 and in Figure 3.2.39 for Ring 10. The degree of saturation of the buffer at the end of the test is plotted in Figures 3.2.41 to 3.2.43. And the final dry density is shown in Figures 3.2.44 to 3.2.46.

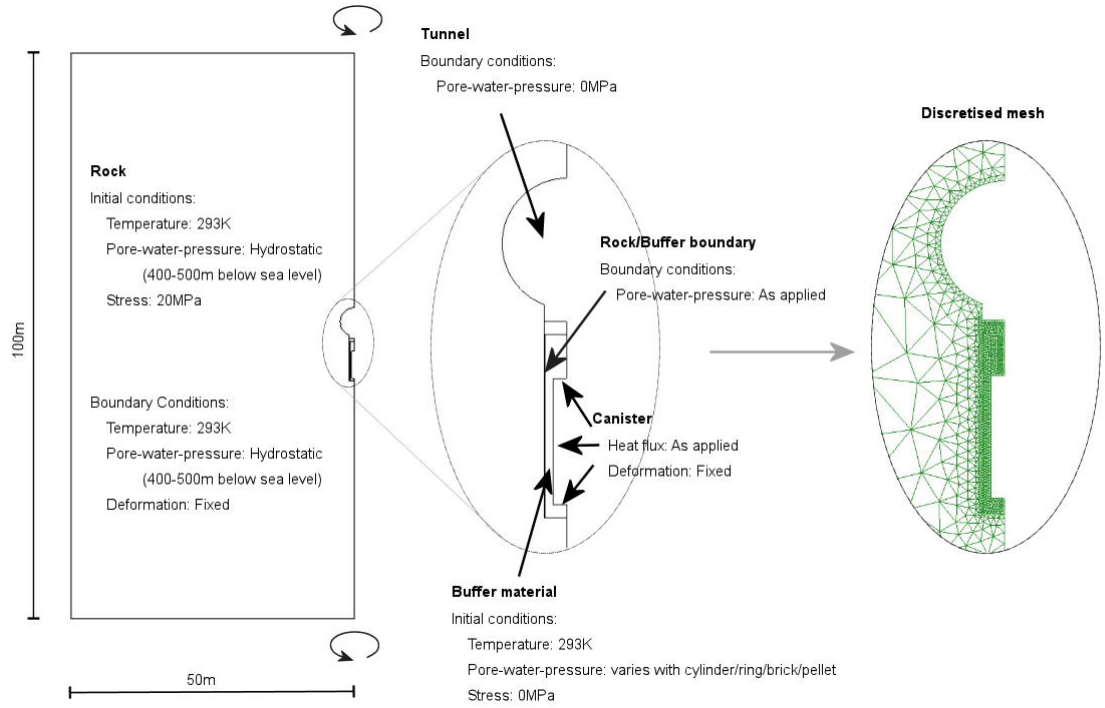

Figure 3.2.32: Domain of the axisymmetric analysis including initial and boundary conditions.

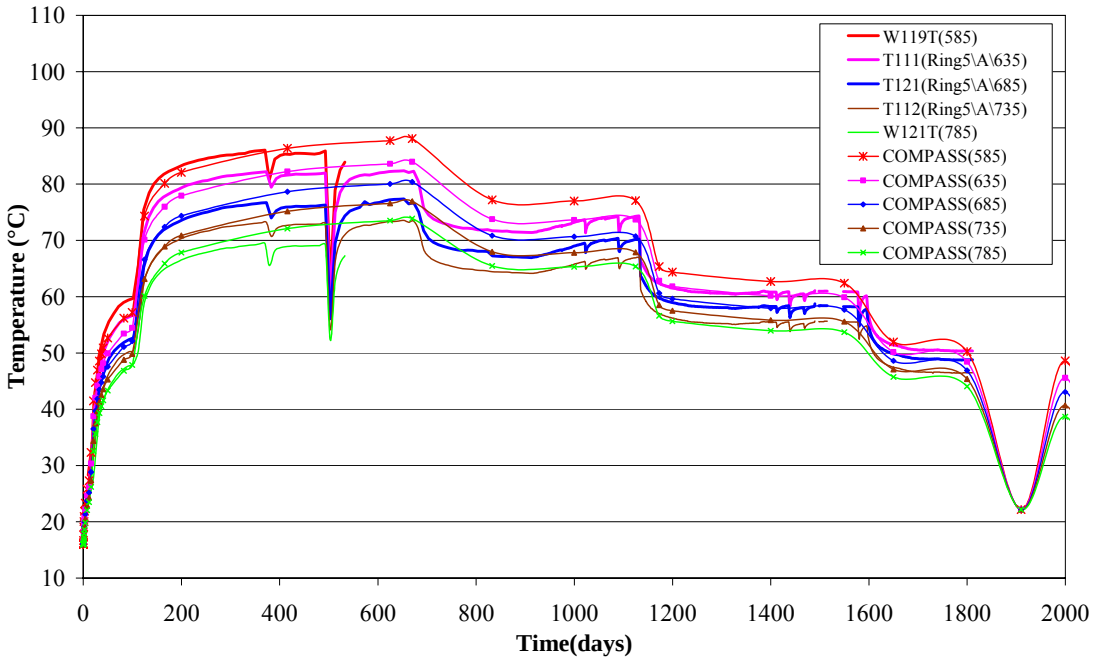

Figure 3.2.33 Comparison of temperature results within R5

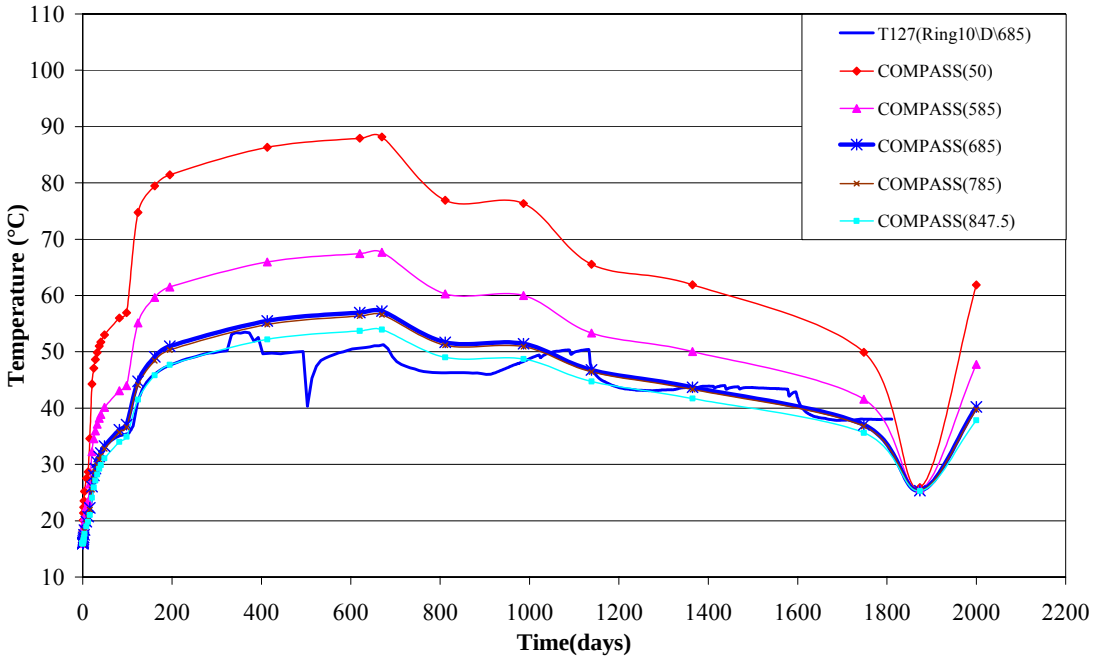

Figure 3.2.34. Numerically simulated temperature results within R10

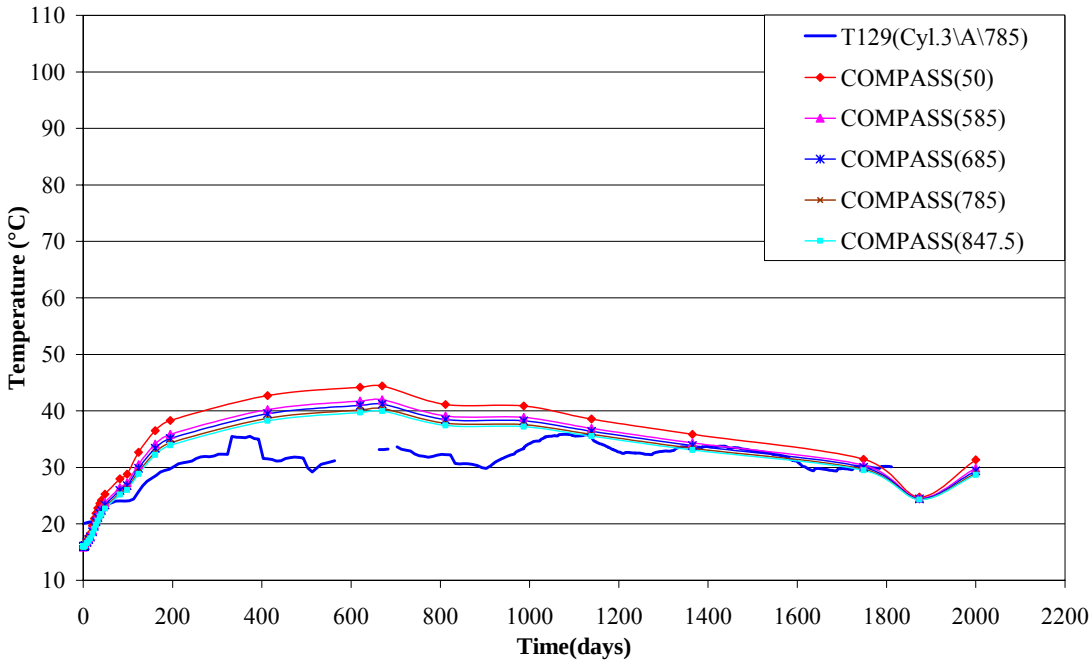

Figure 3.2.35. Numerically simulated temperature results within C3

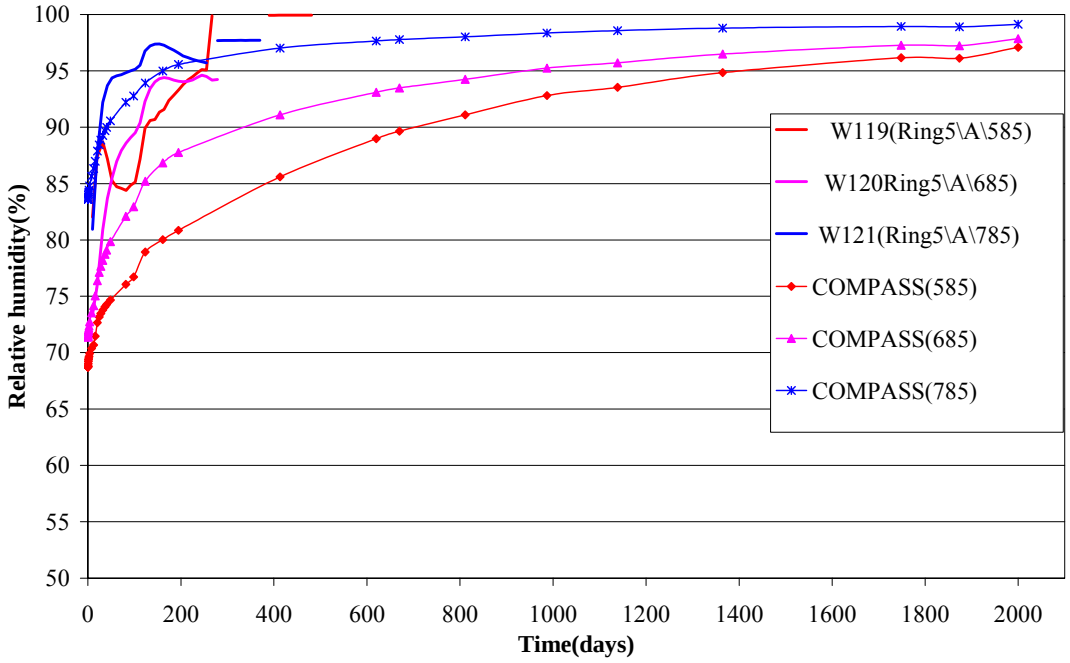

Figure 3.2.36 Comparison of relative humidity results within R5

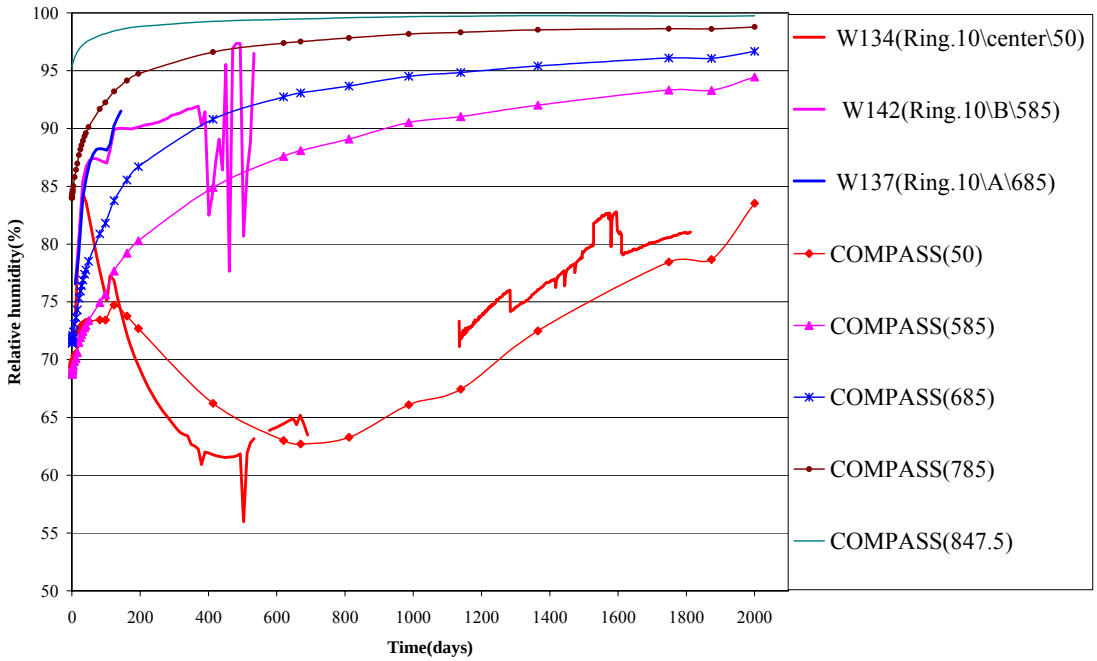

Figure 3.2.37 Comparison of relative humidity results within R10

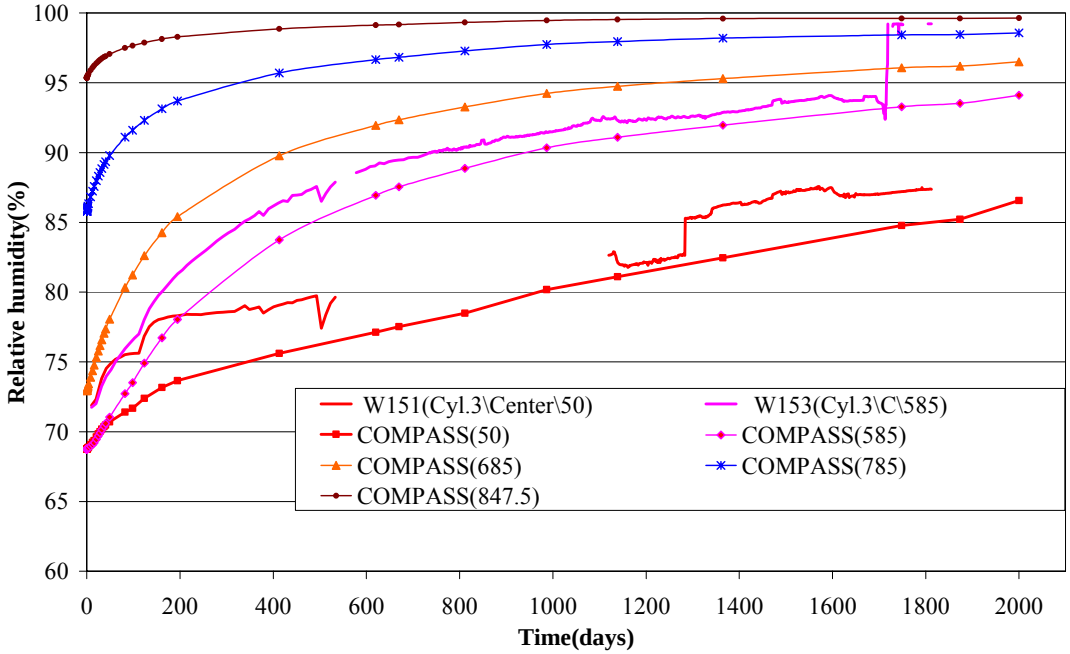

Figure 3.2.38 Comparison of relative humidity results within C3

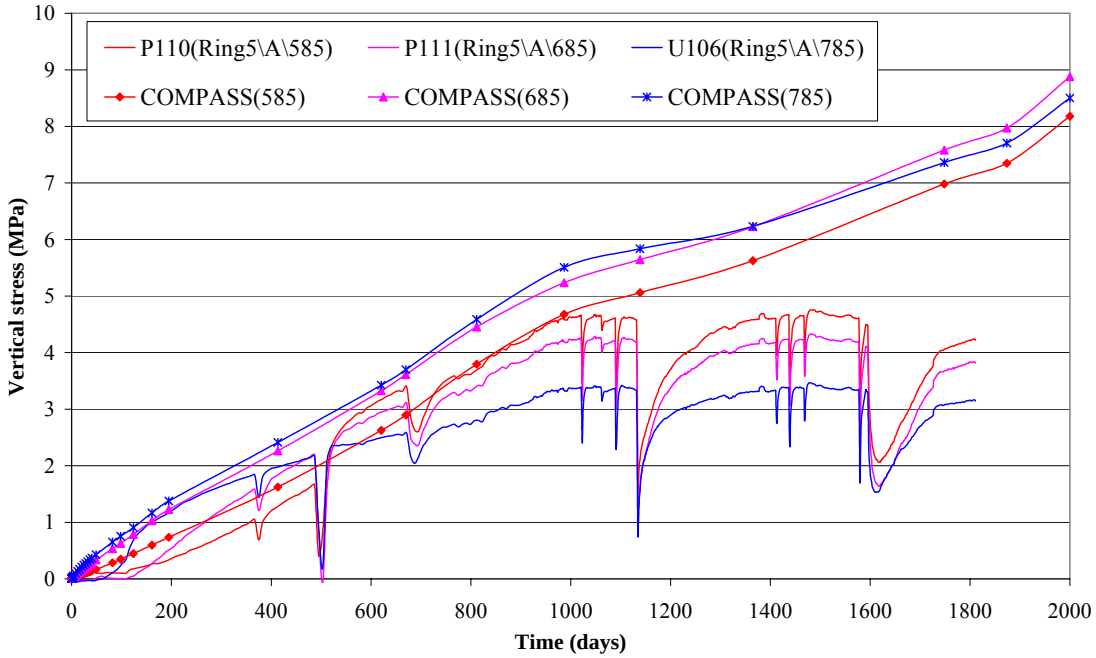

Figure 3.2.39 Comparison of vertical stress results within R5

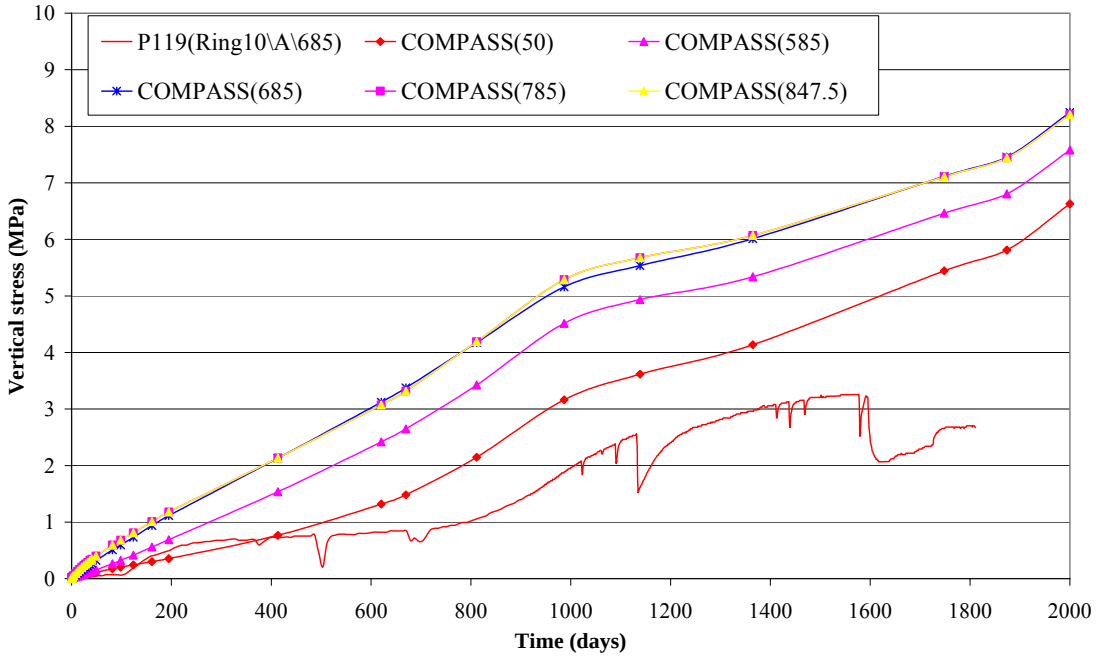

Figure 3.2.40 Comparison of vertical stress results within R10

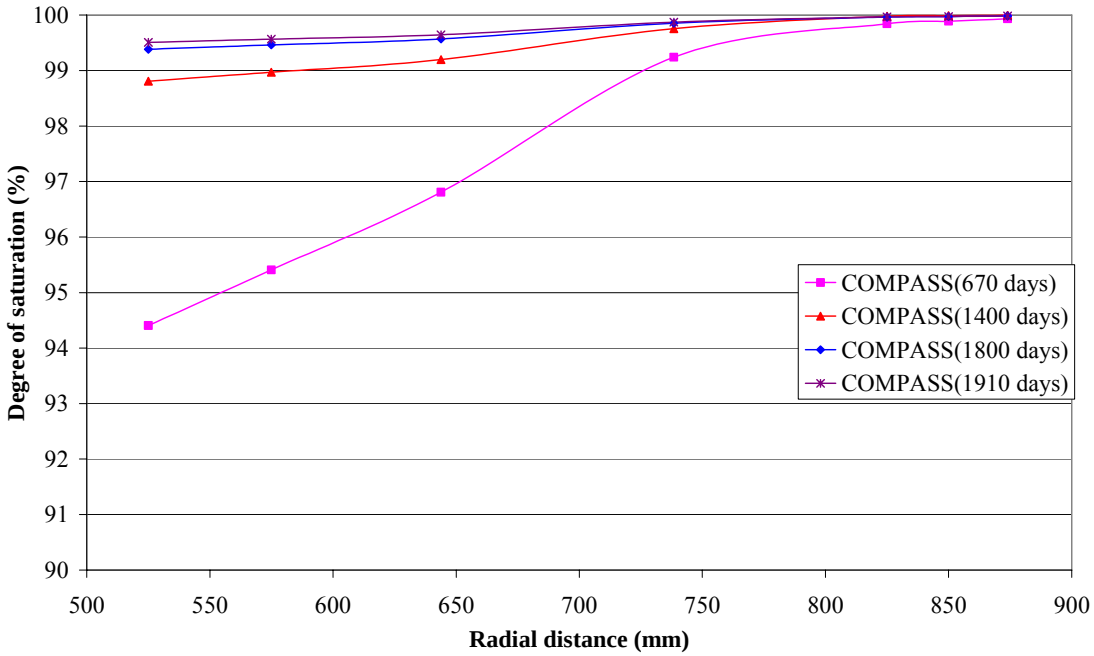

Figure 3.2.41: Numerically simulated degree of saturation profiles within R5

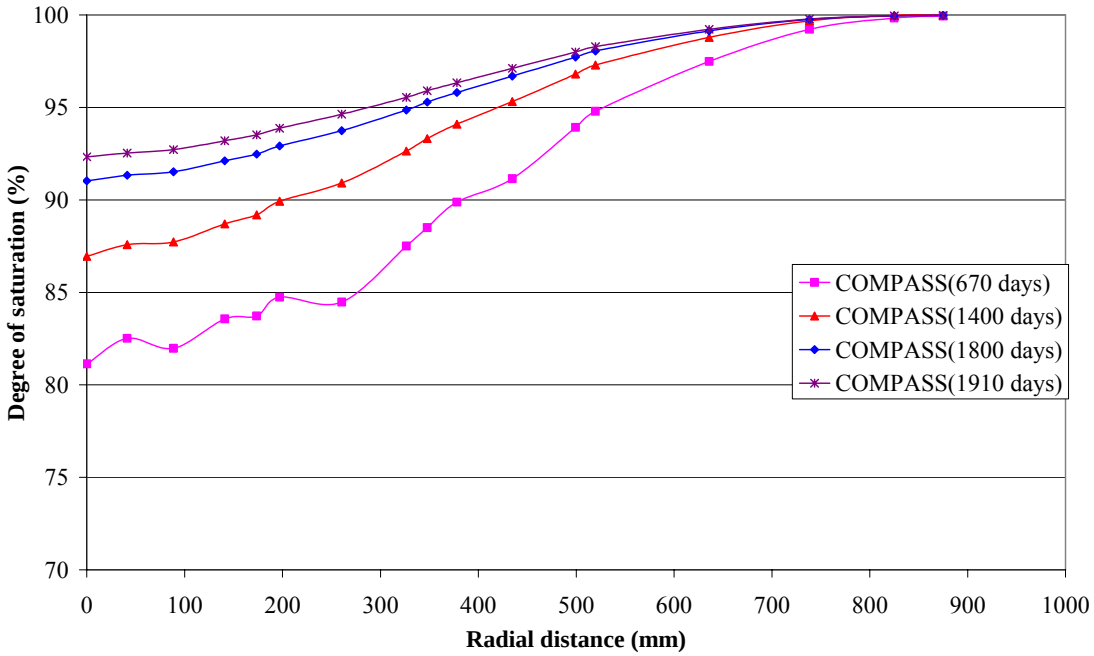

Figure 3.2.42: Numerically simulated degree of saturation profiles within R10

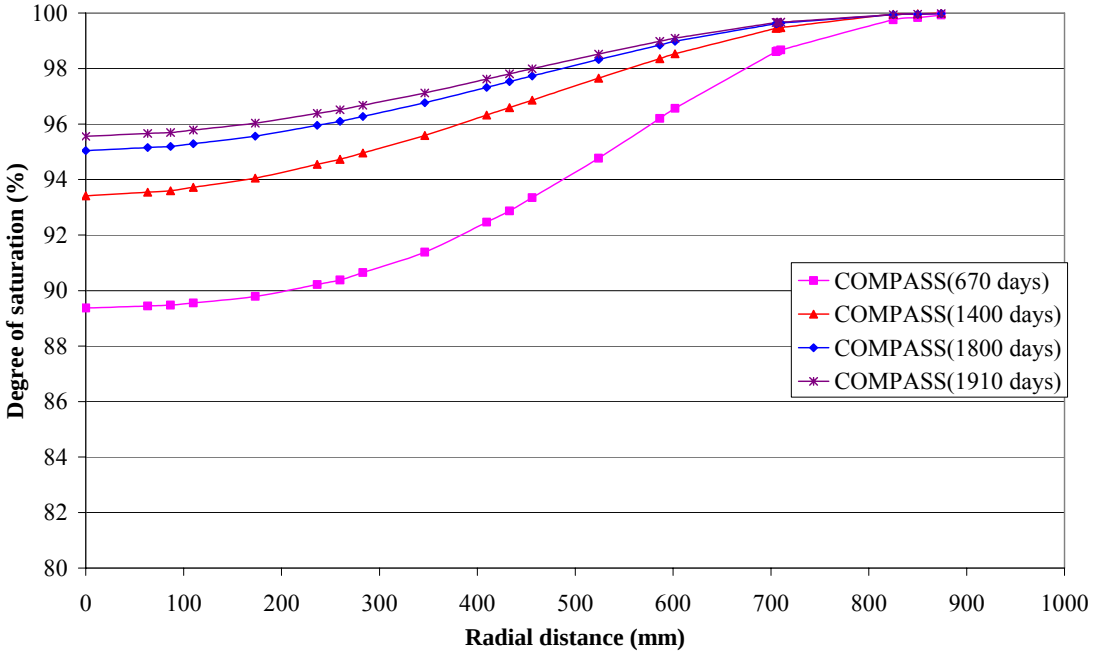

Figure 3.2.43: Numerically simulated degree of saturation profiles within C3

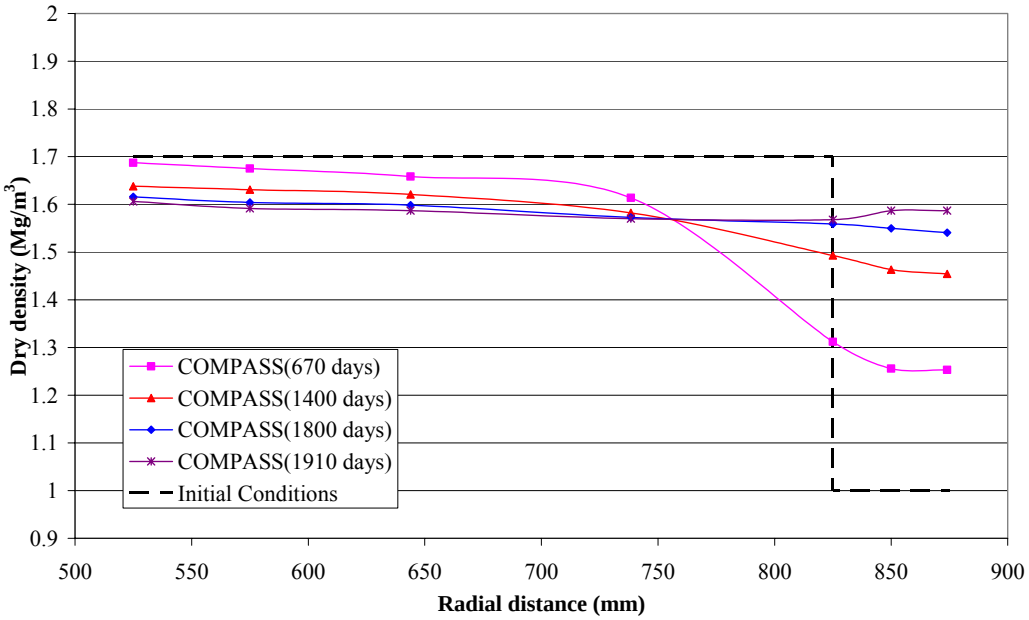

Figure 3.2.44: Numerically simulated dry density profiles within R5

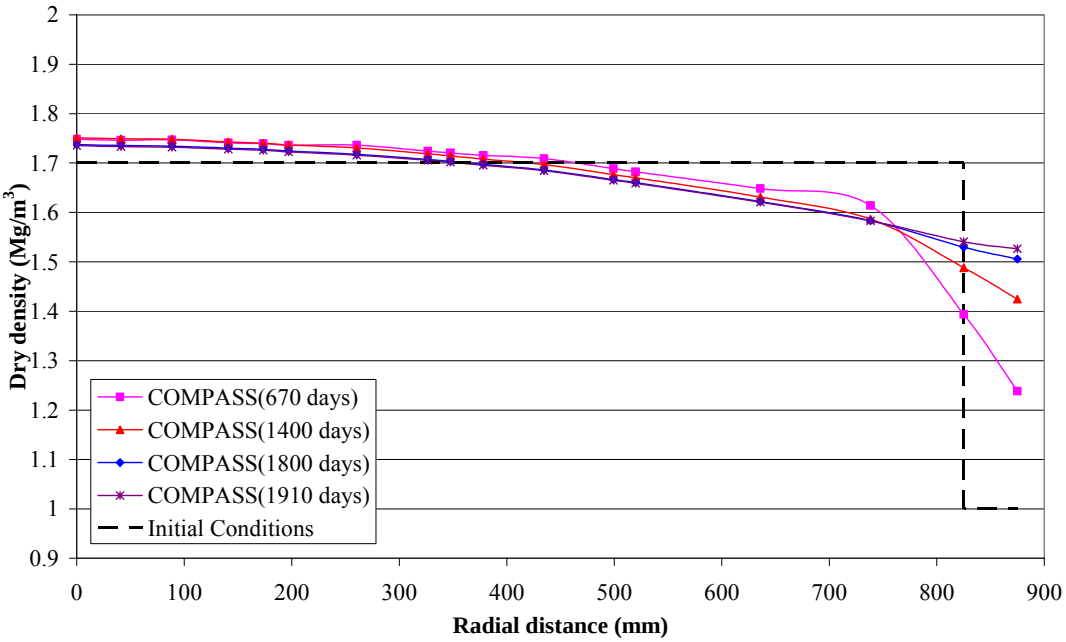

Figure 3.2.45: Numerically simulated dry density profiles within R10

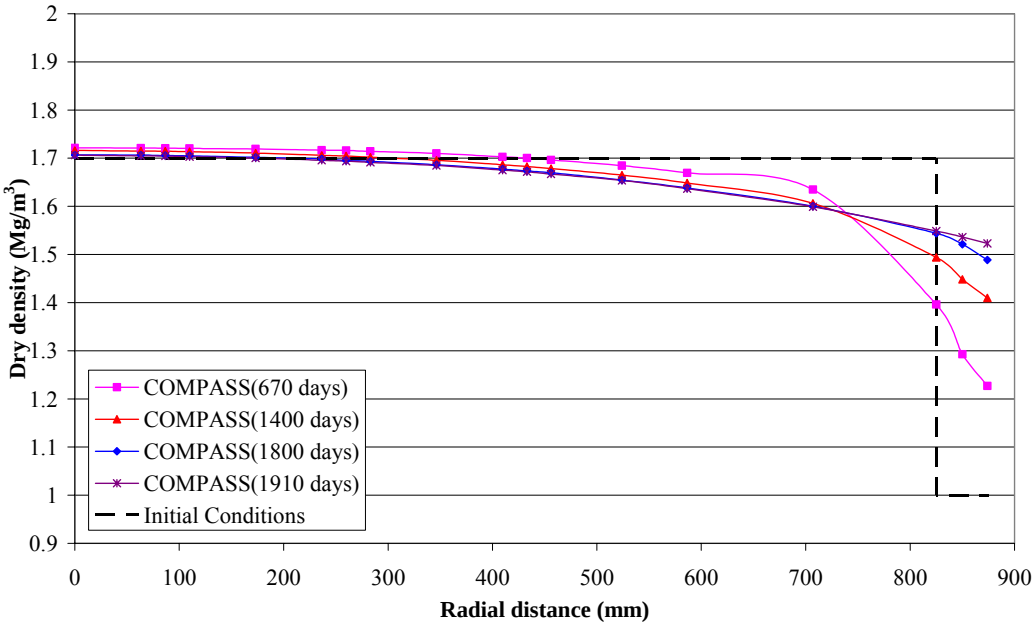

Figure 3.2.46: Numerically simulated dry density profiles within C3

Steady state:

The analysis was continued to steady state conditions under the specified boundary conditions. A lower bound for (local) saturation was found to be 1800 days whereas an upper bound for full saturation was computed to be about 6000 days. However, the final saturation is sensitive to a number of parameters, such as the hydraulic conductivity, the vapour flow law and the definition of full saturation. Saturation may be defined by relative-humidity, degree-of-saturation or suction and, depending on the criterion selected, different results will be obtained. Additionally, the gradients are low close to saturation due to the reduced pore-water pressure gradients and low permeability and, consequently, small changes in the definition of saturation, material parameters or boundary conditions lead to large changes in this time. For example, an increase of 10% in the hydraulic conductivities, which is likely to be within experimental bounds, will yield a reduction in the upper bound saturation time to approximately 4,600 days.

The maximum final radial stress in the rings is predicted, based upon assumptions, to be approximately 7MPa along with the maximum axial stress in the rings of 7.5MPa. In the cylinders the stress level is higher with the maximum radial stress of 10MPa and maximum axial stress of 9.5MPa. The final distribution of the void-ratio is relatively constant throughout the sample.

F. IRSN (CAST3M)

The mesh with the different materials considered (bentonite blocks, bentonite rings, pellets, rock, concrete plug and steel lid) is shown in Figure 3.2.47. For the HM calculation, the rock is not taken into account. In addition, the anchors are modelled by a linear vertical spring located just above the steel lid.

The comparison of temperatures in the buffer is plotted in Figure 3.2.48. The temperature in the rock mass is given in Figure 3.2.49. The comparison of relative humidity is plotted in Figure 3.2.50. The vertical stresses of Ring 5 are shown in Figure 3.2.51. And the comparison of forces in the anchors is plotted in Figure 3.2.52. The dry density of the buffer at the end of the test is shown in Figure 3.2.53

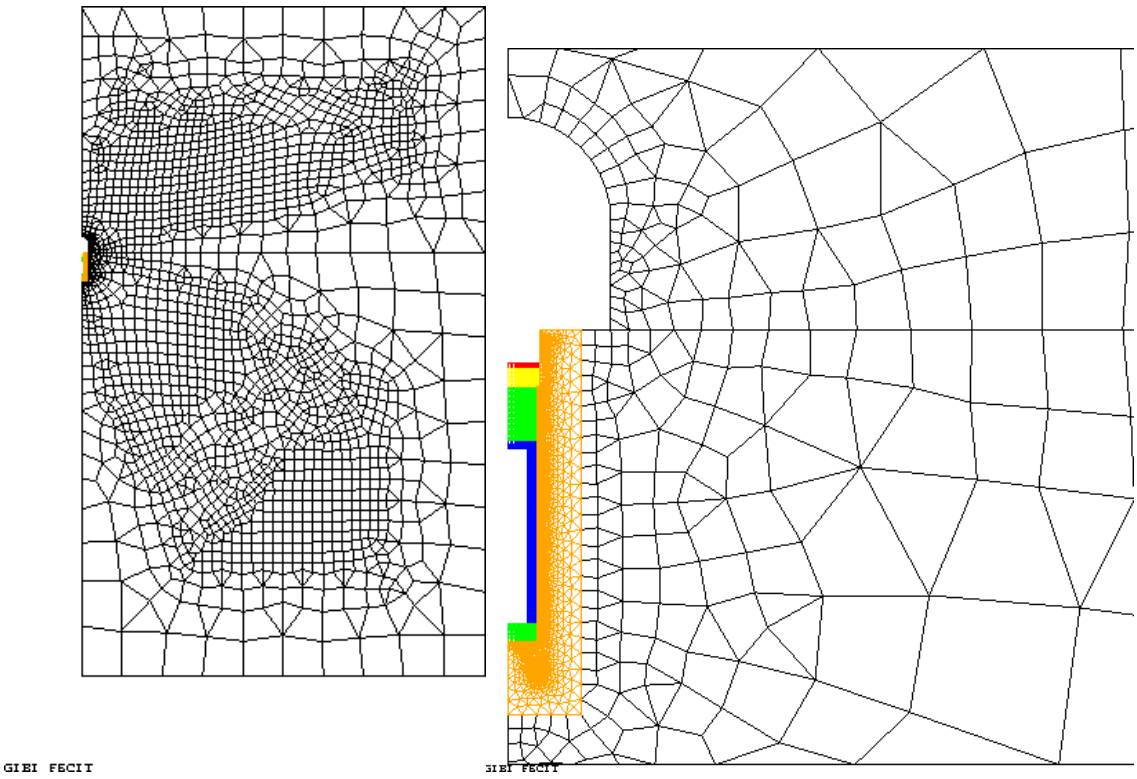

Figure 3.2.47. Total mesh and zoom around the CRT borehole, for the CRT simulation.

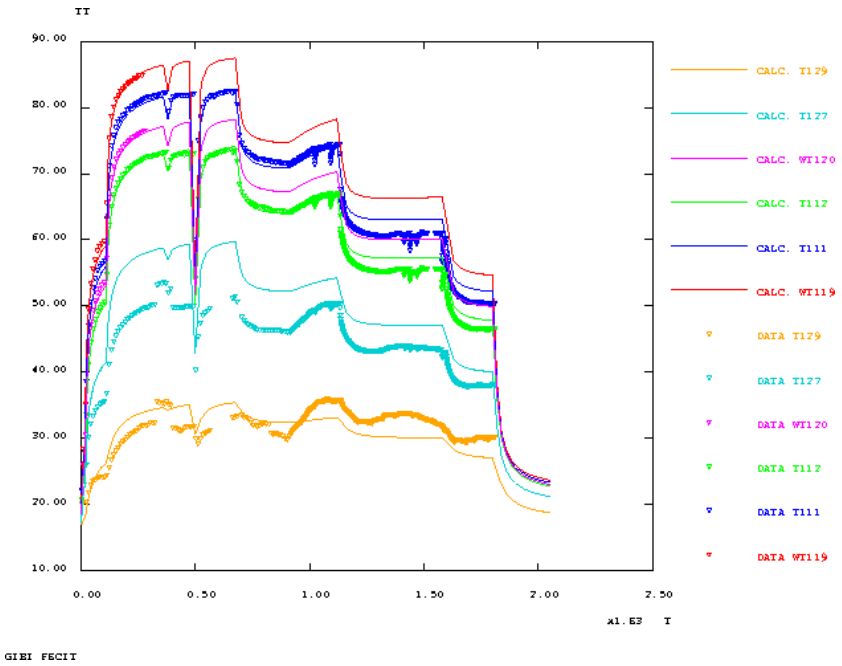

Figure 3.2.48. Comparison of predicted and measured temperatures in the buffer

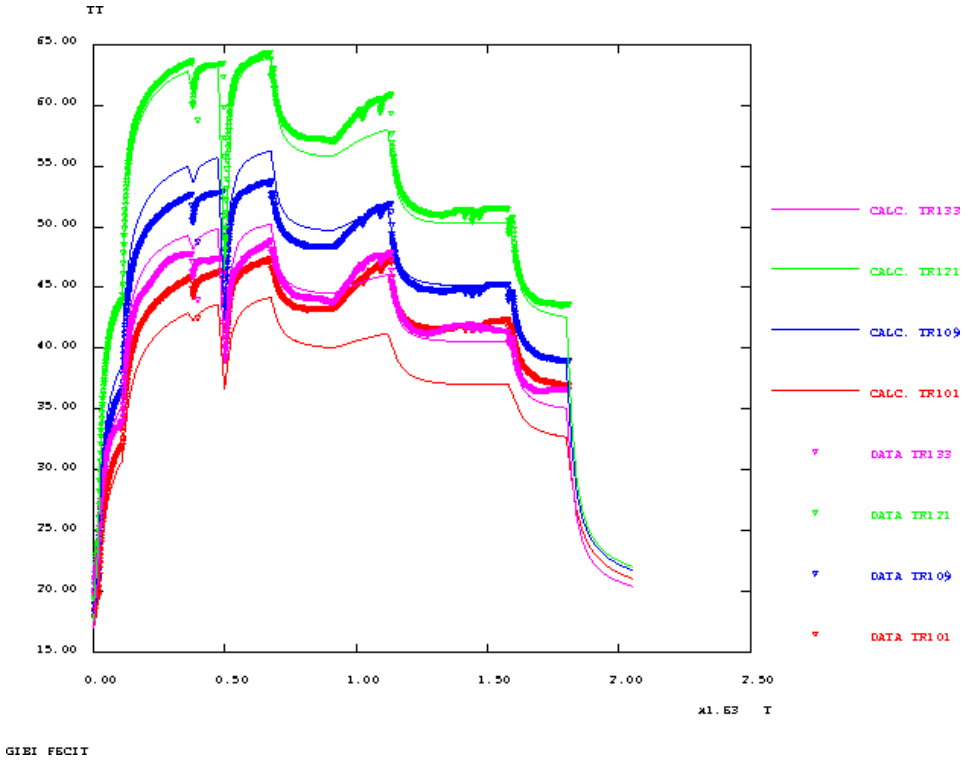

Figure 3.2.49. Comparison of predicted and measured temperatures in the rock mass.

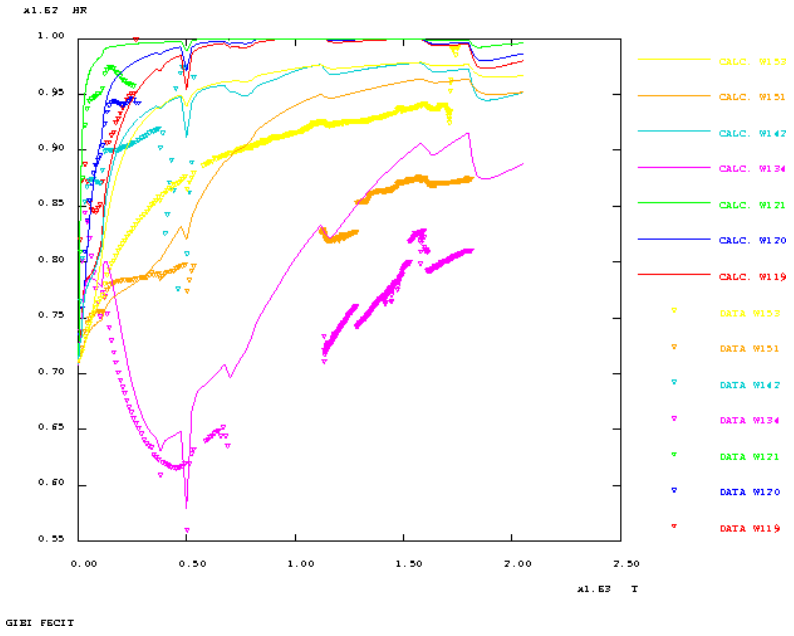

Figure 3.2.50. Comparison of predicted and measured relative humidities in the buffer.

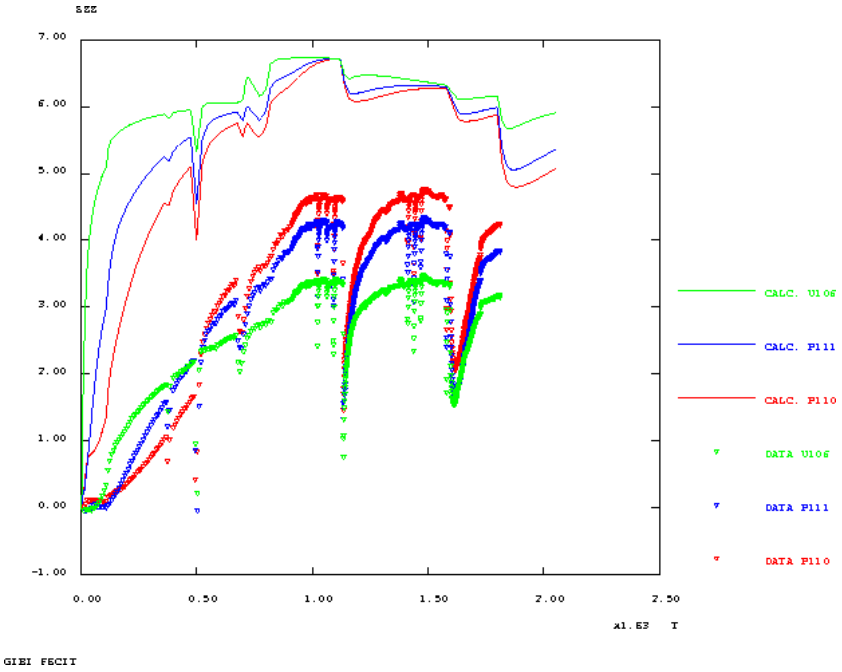

Figure 3.2.51. Comparison of predicted and measured vertical stresses in ring R5.

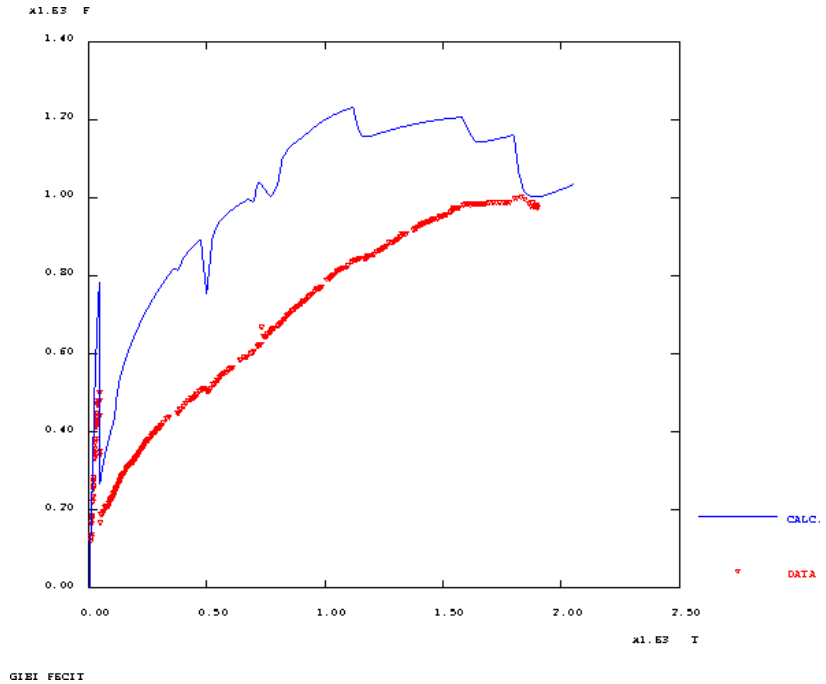

Figure 3.2.52. Comparison of predicted (blue) and measured (red) force in the anchors

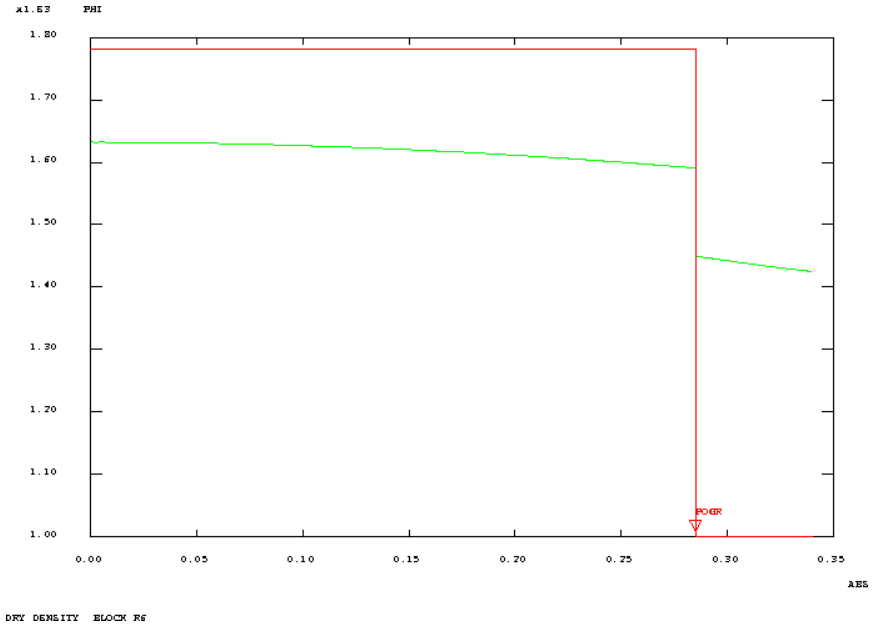

Figure 3.2.53.Comparison of initial dry density initial (red) and final dry density (green) profiles for ring 6.

Steady state: Not simulated

4. Concluding remarks

The modelling of the CRT involved several tasks:

- A 1-D THM analysis focused on a section of the test at a canister mid-height
- A full THM analysis of the entire CRT
- Continuation of the full THM analysis to steady state conditions under specified boundary conditions

The 1-D analysis provided a useful testing ground before undertaking the full THM analysis. By giving prominence to the role of the gaps present in the problem, the modelling of interface behaviour could be more readily studied. Gap properties and evolution were modelled either by specifically developed interface elements or by special continuum elements with 'ad-hoc' specifications. The full THM analysis of the CRT provided the opportunity to demonstrate the capability of the codes developed to simulate a large scale problem. Finally, the extension of the full modelling to steady state conditions gives information on the capabilities of the codes to perform long term analysis as well as to provide parameters related to PA.

In general, the CRT is well simulated by the modelling groups. Even though each group used different formulation and constitutive laws, the overall agreement between observations and calculated values is generally adequate. The following more specific remarks can be put forward:

- Thermal behaviour is universally well accounted for. It is insensitive to constitutive law conditions (conduction governed by Fourier´s law is the dominant phenomenon) but it is sensitive to boundary conditions and modelling geometry. Inclusion of the rock mass in the analysis improves results.

- Hydraulic behaviour is generally adequately reproduced. Drying/wetting, evaporation/condensation and vapour transfer are adequately catered for by the models.

- Hydraulic behaviour, however, appears sensitive to some critical laws and/or parameters: retention curve, relative permeability, gas conductivity. This necessarily reduces the quantitative predictive power of the formulations.

- Successful gap behaviour modelling has been achieved via interface elements or special elements with 'ad-hoc' boundary conditions.

- Homogenization of the dry density of pellets and rings/cylinders was generally successfully modelled by most teams. This is a significant result because it corresponds to the simulation of a novel phenomenon not previously attempted,

one that depends critically on the formulation of the mechanical constitutive law for compacted bentonite and for pellets.

- The reproduction of stress development is uneven between different teams, although the general pattern of swelling stress development is captured by the formulations.

Most teams have continued the full scale analysis until reaching unsaturated state conditions. A number of parameters, related to safety functions such as saturation degree, saturation time, swelling stress magnitude and permeability have been determined by several teams. In general, similar results have been obtained by the different teams, thus increasing the confidence in the reliability of the long term predictions. The performance of the analyses has also revealed the difficultly of pinpointing with precision the time of achievement of steady state conditions. It depends very much on the parameter being examined and on the precise definition of steady state. It is recommended that an operational definition based on PA requirements should be used. From this perspective, steady state conditions can be considered to be reached in a time lying in the interval between 10 and 20 years.

References

Bond, A., P. Maul, D. Savage and J. Wilson (2009), The Use of QPAC-EBS for Project THERESA Full-Scale Tests, QRS-3009A-2, Version 1.0. Quintessa Ltd. UK.

Borgesson, L. (2008). Theresa Project. Canister Retrieval Test.

Gens, A. (2008), THERESA PROJECT - Interface benchmark (1-D): large scale test case. Description of the Canister Retrieval Test (CRT), Centre International de Métodes Numèrics en Enginyeria, Barcelona, Spain.

Lempinen, A. (2009), Simulations of thermo-hydro-mechanical behaviour of the Canister Retrieval Test. Marintel Ky, Finland.

Millard, A. and J.-D. Barnichon (2009), THERESA project, Work Package 4, results for the CRT experiment. IRSN, France.

Thomas, H. R., R.M. Singh and P.J. Vardon (2008), THM modelling of Engineered Buffer at Canister Mid-height related to CRT. THERESA project, Geoenvironmental Research Centre, Cardiff University, UK

Thomas, H. R., R.M. Singh and P.J. Vardon (2009), Thermo-Hydro-Mechanical (THM) modelling of the full Canister Retrieval Test (CRT), THERESA project, Work Package 4, Deliverable 12, Geoenvironmental Research Centre, Cardiff University, UK

Tong, F. (2009), Work Package 4: Coupled Processes in Buffer and Rock-Buffer, Interfaces. The Report on Simulation of CRT. Royal Institute of Technology, Stockholm, Sweden.

Zandarín, M. T., S. Olivella, E. Alonso & A. Gens (2008), THERESA project, Report nº 2: Interface Benchmark (1-D). Centre International de Métodes Numèrics en Enginyeria, Barcelona, Spain.

Zandarín, M. T., S.Olivella & A. Gens (2009), THERESA project, Canister Retrieval Test, Large scale test case. Centre International de Métodes Numèrics en Enginyeria, Barcelona, Spain.